

STUDY OF MIXED, HETEROGENOUS FLOW
KINEMATICS OF POLYMER MELTS
IN CONVERGING CHANNELS

By

SUNIL SINGH AJAI

Bachelor of Technology

Bharatiar University

Coimbatore, India

1990

Submitted to the Faculty of the
Graduate College of the
Oklahoma State University
in partial fulfillment of
the requirements for
the Degree of
MASTER OF SCIENCE
December, 1992

Thesis
1992
A312x

STUDY OF MIXED, HETEROGENOUS FLOW
KINEMATICS OF POLYMER MELTS
IN CONVERGING CHANNELS

Thesis approved :

Alan Lee

Thesis Adviser

James R. Whithy

Arland H. Johannes

Thomas C. Collins

Dean of the Graduate College

ACKNOWLEDGEMENT

I wish to express my sincere thanks and gratitude to my major professor, Dr. David A. Tree, who guided my path all along on my thesis as adviser and did not stop short of advising me in every aspect. I also thank him for providing me with an opportunity to work on polymers and to give me a feel and better understanding of the subject.

I would like to express my sincere gratitude to my parents and family members for having encouraged me to pursue my masters degree abroad and also for their consistent motivation, caring and continuous support. I salute the man who always felt that life was incomplete without a proper education. I would also like to express my gratitude to my fiancée, nsk, for her understanding, love and enormous patience. I thank all my friends for their consistent encouragement which always kept me going.

I am thankful to the School of Chemical Engineering, Oklahoma State University, for assisting me with liberal funds for most of my stay here.

TABLE OF CONTENTS

Chapter	Page
I INTRODUCTION	1
Polymer Rheology	1
Converging Flow	2
Thesis Organization	3
II BACKGROUND	4
Converging Flow	4
Flow Birefringence	10
Polymer Rheology	16
Kinematics	16
III EXPERIMENTAL	22
Material	23
Equipment	23
Slit Flow Die	23
Optical and Video Setup	26
Technique and Procedure	28
Rheological Data	28
Stress Optic Coefficient	30
IV RESULTS AND DISCUSSIONS	32
Stress optic Coefficients	32
Rheology	45
Converging Section	45
V SUMMARY, CONCLUSIONS AND RECOMMENDATIONS	59
Summary and Conclusions	59
Recommendations	60
BIBLIOGRAPHY	61

APPENDIXES

APPENDIX A - NOMENCLATURE	66
APPENDIX B - STRESS OPTIC COEFFICIENT	69
APPENDIX C - MIXED FLOW KINEMATICS	73
APPENDIX D - DESIGN CONSIDERATIONS OF THE DIE	80
APPENDIX E - APPARATUS DESCRIPTION	84

LIST OF FIGURES

Figure	Page
3.1: Various sections of the Slit Flow Die	24
3.2: Optic and Video Setup	27
4.1: Slit Flow Birefringence Pattern at 150 °C and $\alpha = 0$	34
4.2: Slit Flow Birefringence Pattern at 150 °C and $\alpha = 30$	35
4.3: Steady State Pressure Gradient at 150 °C and 9 RPM	37
4.4: Birefringence Pattern in the Converging Section at 150 °C, RPM = 7, and $\alpha = 0$	38
4.5: Calibration of C at 150 °C	40
4.6: First Normal Stress Difference at 150 °C	43
4.7: Shear Stress as a Function of First Normal Stress Difference	44
4.8: Natural Log of CT as a Function of Inverse Temperature	46
4.9: Stress Field Distribution of LLDPE at 150 °C, RPM = 7	48
4.10: First Normal Stress Difference in the Converging Section at 150 °C, RPM = 7	50
4.11: Elliptical-Cylindrical Coordinates	51
4.12: Tracer Particle Analysis at 150 °C, RPM = 7	53
4.13: Ψ_c as a Function of c	56
E.1: Apparatus Setup	86

LIST OF TABLES

Table	Page
3.1: FLOW GEOMETRIES OF PARTICULAR IMPORTANCE (10)	7
3.2: RELATIONSHIP OF THE STUDIES OF CONVERGENT FLOW (10) . . .	8
4.1: VARIATION OF STRESS OPTIC COEFFICIENT WITH TEMPERATURE	41
4.2: VALUES OF Ψ_c AS A FUNCTION OF c FOR LLDPE AT 150 °C AND 7 RPM	55
B.1: STRESS OPTIC COEFFICIENT AT 140 °C	70
B.2: STRESS OPTIC COEFFICIENT AT 150 °C	71
B.3: STRESS OPTIC COEFFICIENT AT 170 °C	72
C.1: DATA ALONG A PARTICULAR STREAMLINE AT $\eta = 78.1$	74
C.2: DATA ALONG A PARTICULAR STREAMLINE AT $\eta = 76.2$	75
C.3: DATA ALONG A PARTICULAR STREAMLINE AT $\eta = 85.4$	76
C.4: DATA ALONG A PARTICULAR STREAMLINE AT $\eta = 78.5$	77
C.5: DATA ALONG A PARTICULAR STREAMLINE AT $\eta = 81.1$	78
C.6: DATA ALONG A PARTICULAR STREAMLINE AT $\eta = 82.6$	79

CHAPTER I

INTRODUCTION

The significance of polymeric materials in the modern world has been tremendous. Plastics and polymers touch us in almost every act of daily life. Due to their superior properties over many materials and their ability to meet several particular service requirements and applications, the demand for more new polymeric materials is on the increase thereby rapidly fueling the growth of polymer industry. Although a wide range of materials have been developed, the need for new polymeric materials has been constantly felt. Among the many issues associated with polymeric materials, one of the most important is their flow behavior. Hence, knowledge of polymer melt rheology, which has been the prime focus of this thesis work, is essential for any processing related activities.

Polymer Rheology

The relation between the deformation or the deformation rate of a fluid and the forces acting on the fluid is a constitutive equation or the rheological equation of state, and is critical to the design of any polymer process (34). Empirical observations and/or a molecular model of polymer behavior govern the development of any rheological equation. Many practical processing conditions are in the regime where both extension and shearing takes place

simultaneously, with the additional characteristic that the magnitude of the deformation rate is spatially dependent. Rheological equation of states usually account for the flow behavior of polymers either in extensional or shear flow, but rarely both at the same time. Hence correction factors are often employed to account for the deviation from idealized behavior, which at times can lead to significant errors.

The ideal would be a single, simple equation of state based on a realistic molecular model. Such a model does not exist at present (34). A rheological equation of state which suitably describes the kinematics of a polymer melt given its applied stresses in mixed flow conditions would be helpful from a practical as well as a theoretical point of view.

Converging Flow

The converging flow of viscoelastic fluids has been a subject of considerable interest to both theoretical and experimental rheologists. From the theoretical point of view the converging flow field provides an opportunity to test the potential usefulness of various rheological equations of state. From a practical point of view, a better understanding of the flow behavior of polymeric liquids, in particular polymer melts, in the converging flow field is very important to the success of various polymer operations such as plastics extrusion, film extrusion, etc.. Therefore a better understanding of the flow behavior of polymer melts in converging flow fields is essential.

Many theoretical studies have been limited to simple flow situations such as

steady simple shearing flow or steady Poiseuille flow; that is, they have been limited mainly to viscometric flow problems. Also, most of the experimental apparatuses available today for the determination of rheological properties are based on a viscometric flow field. This is not surprising when one considers the mathematical complexities that arise even from relatively simple rheological equations of state in simple shearing flow.

Therefore a study and understanding of polymer behavior in channels acquires considerable significance.

Thesis Organization

This thesis has been divided into five chapters. The theoretical development and relevant background information concerning polymer melt rheology and converging flow is discussed in Chapter II. A detailed description of the experimental apparatus and materials used, along with the procedure is given in Chapter III. A discussion of the data obtained is presented in Chapter IV. Chapter V summarizes the results and presents comments on the recommended direction of continuing work in mixed, heterogenous flow of polymer melts in converging channels.

CHAPTER II

BACKGROUND

The study of mixed, heterogenous flow kinematics in polymer melts, by rheo-optic techniques, requires a background in several subjects including: flow through converging channels, flow birefringence, and rheology. Each of these subjects has a rich literature; the relevant portion of which is discussed in this chapter.

Converging Flow

One of the most important non-viscometric flow geometries for non-Newtonian fluids is the flow from a reservoir or a pipe to a tube of smaller diameter. Such a flow field is encountered in many industrial process involving polymer melts and solutions. Of the numerous methods available for flow of polymer melts from a reservoir to a tube, two often most commonly used methods are: (a) flow through a sudden contraction and (b) a tapered die entrance.

Tapered dies are generally preferred in extrusion for two reasons. The first advantage being to avoid recirculation zones in the corners of the reservoir section above the die entrance, due to the non-linear viscoelastic nature of the melt. It has been found in most cases in tapered dies, that there is no

recirculation zone. In industrial processing, some polymers (PVC, Nylon 6) form crosslinkages or degrade when they stay in the stagnation zone caused by the recirculation, which is detrimental to smooth operation. Dies with tapered entrances eliminate this problem. The other reason for the use of tapered dies, equally important as the first, is that a die with a tapered entry can yield an increase in productivity by permitting operation at higher flow rates (due to decreased pressure drop). At higher flow rates melt flow instability or "melt fracture", starts to occur thereby severely hampering the process. Thus the study and analysis of converging flow has been of considerable significance. Although our interest in converging flow is altogether different than the interest of most previous investigators, vast study of vortex formation has provided valuable information, regarding their characteristic, for this study.

An ideal die is one which maximizes the output rate of smooth extrudate and minimizes pressure drop and swell ratio. Such a die would permit a comprehensive study of general features like stress-strain relations and velocity profiles of entrance flows. Such optimization commonly requires an proper choice of taper for the converging region in the die.

The kinematics of the entrance flow problem are complex and the deformation rates vary widely throughout the flow field. The most direct method of analyzing such a problem is the application of finite differences or weighted residuals to solve the equations of motion and continuity in conjunction with an appropriate constitutive equation.

Attempts to characterize the flow of non-Newtonian fluids through

converging channels have been done in the past. Four flow geometries of particular importance have been identified. These are shown in Table 1 (10). Measurements involving free convergence, constrained convergence (both lubricated and unlubricated), and opposing jet flows are illustrated. In free convergence the accelerating column of fluid approaches the die inlet between rotating vortices. In constrained convergence, the angle of convergence is restricted by the walls of the die. The die may be unlubricated in which case the boundary layer next to the wall is assumed to have zero velocity. This produces the velocity profile which includes both shear and elongation. In the special case of constrained convergence where the wall is lubricated, no shear flow occurs.

The relationship of studies of convergent flow associated with stretching (irrotational) flow has been compiled in Table 2 (10). Table 2 illustrates two main development of thoughts viz. free convergence from the reservoir to the die and constrained convergence. The flow behavior of Newtonian fluids and polymer melts in free and constrained convergence, primarily as in stretching flow, for different geometries has been discussed in the Table. Bridging the two thoughts is the study of stress distribution carried out by Drexler and Han (27). The study of opposed jets was separately carried out by Mackley.

Study of flow from a channel of larger cross section to another of smaller cross section has been cited in literature by many studies. Bagley (25) in 1957, employed very large entrance flow corrections to account for polymer melts. Tordella was among the earliest to employ the optical properties of polymer

TABLE 3.1
FLOW GEOMETRIES OF PARTICULAR IMPORTANCE (10)

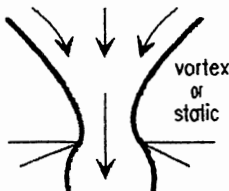

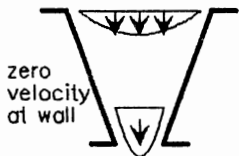
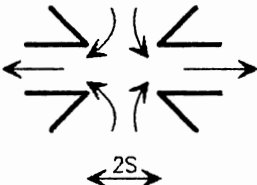
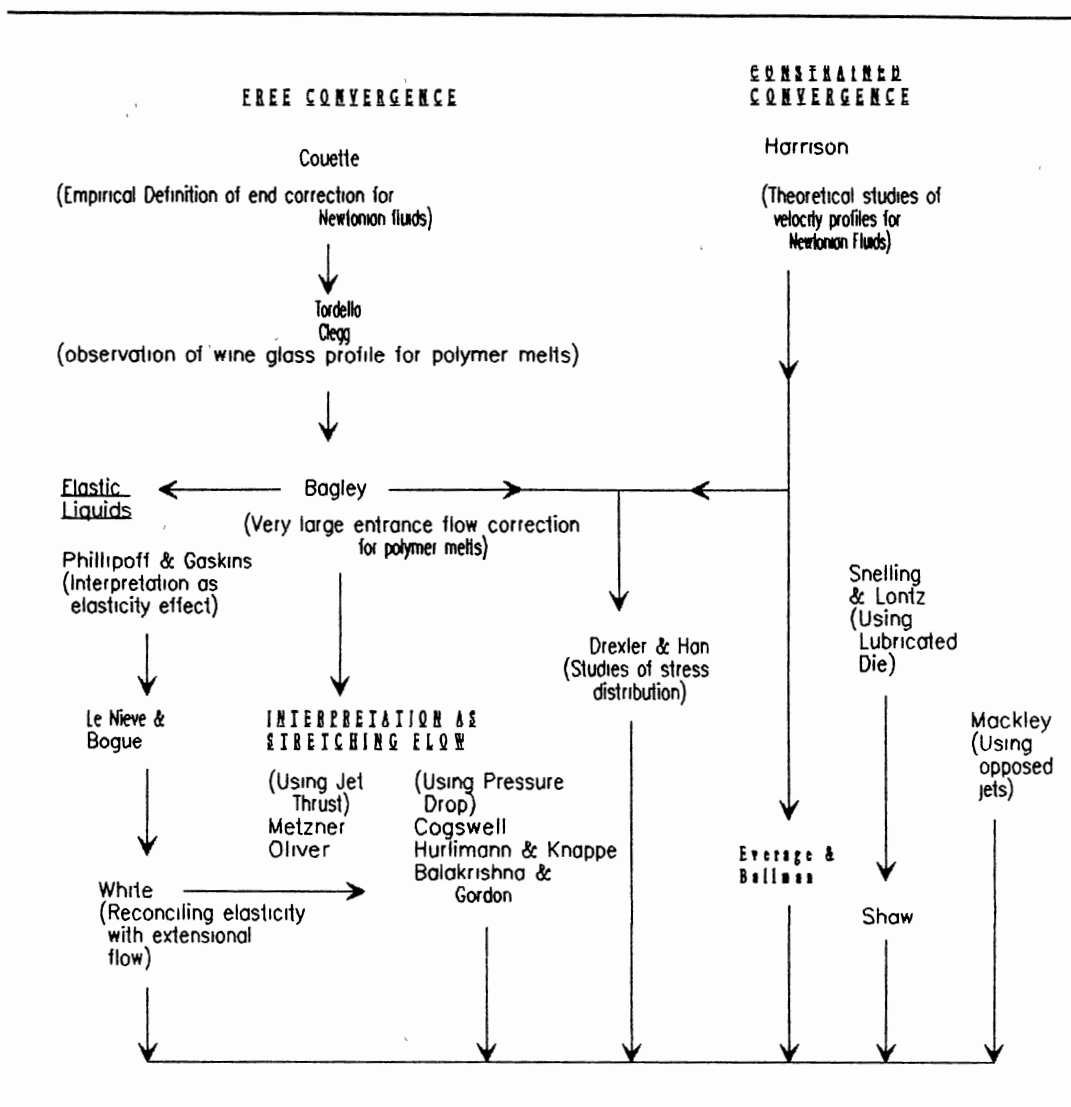
DESCRIPTION	GEOMETRY	MEASUREMENTS
Free convergence		Pressure drop P_0 Half angle of convergence θ Die radius r Flow rate Q Swell ratio B Jet thrust
Constrained convergence		Pressure drop P_e Half angle of convergence θ Die radius entry r_0 exit r_e Flow rate Q
Constrained convergence (unlubricated)		θ , r_0 , r_e , Q as above
Opposed jets		Distance between jets $2S$ Die radius r

TABLE 3.2
RELATIONSHIP OF THE STUDIES OF CONVERGENT FLOW (10)



melts and carried out experimentation on flow visualization.

Point by point analysis for shear stresses and the normal stress difference was carried out by Adams et al. (24) using the birefringence technique. Similar studies were carried out by Fields et al. (5) and Yoo and Han (11) and found that the distribution of wall normal stresses goes through a minimum and that the extensional stress along the centerline of the converging channel goes through a maximum.

The importance of a fluid's extensional properties relative to its shear properties, in determining entry flow behavior, was shown by White and Baird (17), who concluded that the vortex growth was a material dependent function of Weissenberg number (ratio of time characteristics of a polymer).

Subramanian et al. (23) studied converging flow of polymer solutions and showed that the Goddard-Miller model agreed quite well with the measured data. However, the work of Subramanian et al. would not be of great assistance to this work because polymer solutions behave very differently from polymer melts.

The study of velocity profiles in converging flows has been of considerable interest. The effect of varying flow rates on the velocity profiles has been discussed by Ballenger and White (19) who observed stagnant circulating regions in the corners of the die when the flow rates were increased. Drexler and Han (8) made velocity measurements using the technique of streak photography, the accuracy of which is restricted by the curvature of the streamlines.

Another issue associated with the velocity profile is the pressure drop along the channel. Boles et. al (6), Ballenger et. al (19), Duda et.al (7), Gibson and Williamson (16), and Han (13) etc. have studied the influence of die geometry on the pressure drop and concluded that in polymer melts the pressure drop occurs almost entirely upstream of the constrained convergence entrance and that the flow profile is largely developed by the time the fluid has arrived at the mouth of the tube. Cogswell (4,10) has made a detailed analysis of polymer melts in converging flow for both conical-cylindrical and wedge shaped dies by distinguishing the shear stress and elongation stress and deriving explicit equations for these quantities. Hurlimann (53), Metzner and Balakrishna (54), Oliver (55), and Han (10) developed relations for elongation strains in converging flows and found that very small errors occurred in their calculations upto a die angle of 30° .

Flow Birefringence

For years the photoelastic technique has been a powerful tool for experimental stress analysis in solids. This technique is based on the fact that certain substances become temporarily, doubly refracting (ie., anisotropic to the passage of light) when subject to stresses. When a doubly refracting substance is viewed by transmitted light between two polarizing plates, visible interference patterns are produced, which are related to the material dimensions, properties, and to the stresses in the specimen. A complete treatment of the photoelastic theory is given by Frocht (31), Durelli and Riley

(32), and Hendry (33).

The earliest such phenomena in liquids was reported for solutions by Maxwell (45) in 1873, and has since then been subjected to intense investigation. In liquids, the phenomenon is called streaming birefringence, streaming double refraction, or flow double refraction.

The application of flow double refraction was largely restricted to study of molecular size and shape before Humphry (43) in 1923 showed the possibility of using doubly refracting liquids as tools for the visual analysis of flow. However the first attempt to quantitative measurements of stress profiles with flow double refraction was made by Alcock and Sadron (44). In 1952, Rosenberg (46) by careful study of fluid flow showed that the direction of maximum shear stress in fluids and the direction of the streamlines are not coincidental except for the case of parallel streamlines.

Prados and Peebles (26), Bogue et. al (24), Han (28), Yoo and Han (29), Okubo et. al (21), and Ballenger et. al (17) calculated the stress by point by point analysis in channels of different geometries using the birefringence techniques. They showed that the distribution of wall normal stresses goes through a minimum and that the extensional stresses along the centerline of the converging channel, determined from the stress birefringence pattern, go through a maximum.

A long standing problem associated with the birefringence technique was its diffused nature of the isoclinic bands. An explanation for the isoclinic band spreading in a 2D slit flow geometry was given by McHugh et al. (30).

McHugh et al. showed that the band spreading is attributed to the positional dependence of shear stresses in the vicinity of the side wall viewing windows, leading to a range of positions along the channel depth at which a given stress level may exist. They also showed that for a given rotation of the polars, the inside line of the resulting band represents the stress characteristics of the 1D centerline flow to be used for the evaluation of the isoclinic angle. However, Tree (34) with the help of digitized data showed that the position of isoclinics does not correspond exactly to the inside edge but slightly beyond this point. Galante and Frattini (57) utilized the differential propagational Mueller matrix formulation to calculate the retardance and the isoclinic angle. Galante and Frattini showed that negative deviations of a few percent occur in retardation when the aspect ratio is ten. Also the retardation errors increase with elasticity and flow rates and vary inversely for small aspect ratios.

In general the applicability of flow birefringence has been used to study the presence of frozen in stresses in articles made by dies of complex geometries. Since this technique has better compliance times and does not interfere with the flow, birefringence is often preferred over mechanical methods (35).

However, the experimental technique required to carry out birefringence studies has some limitations. First, the flow channel should have flat surfaces through which a light beam passes; second, as the flow rate is increased, the number of fringes also increases, making the identification of different fringe orders very difficult.

The use of flow birefringence as a method to treat viscoelastic fluids was

first suggested by Lodge (49), followed by extensive experimentation by Phillippoff (56) to extend the stress optical rule from liquids to solids and concentrated polymeric solutions. Janeschitz-Kriegl (35) made a comprehensive review of the molecular theory evolving out of these studies with dilute polymer solutions.

Birefringence refers to the differences in the refractive indices along the two principle axes of a material. In solid photoelasticity it has been envisioned that when polarized light enters an optically anisotropic medium, the beam splits into plane polarized components (the ordinary and extraordinary beam) in the direction of the principal optical axis which travel along these axes at different speeds. When the two components emerge from the medium, they have a certain relative path difference, R , given by

$$\Delta n = R\lambda/L \quad (2.1)$$

where L - the thickness of the medium
 λ - the wavelength of light
 Δn - the difference between the first and second principle refractive indices.

It has been shown that when the direction of the light path is made to coincide with the direction of one of the principle stresses, say τ_{p3} , the relative retardance (or fringe order) can be related to the difference in the other two principle stresses, $\Delta \tau$ by

where C is the stress optic coefficient.

$$\Delta n = C \Delta \tau \quad (2.2)$$

This empirical relationship known as the stress optic relationship (SOR) was primarily due to the work of Newmann and Maxwell (45). While deriving this relationship two assumptions have been considered. They are, (i) the principle axes of the stress tensor is collinear with the principle axes of the refractive index tensor or mathematically :

$$\chi_m = \chi_o = \chi \quad (2.3)$$

where χ_m - orientation angle of stress tensor

χ_o - orientation angle of refractive index
tensor

χ - isoclinic angle

and (ii) the birefringence at any point is linearly proportional to the first principle stress difference in the plane perpendicular to the axis of light propagation ie.

$$\Delta n = C [\tau_{p1} - \tau_{p2}] . \quad (2.4)$$

The validity of the linear assumption has been showed by several studies, particularly at low deformation rates (31, 32, 33). Extensive work on birefringence has been carried over by Janeschitz-Kriegl (35), Wales (36) and many others on LDPE undergoing simple elongation at constant temperature and strain rate and found that the SOC ranges between $1.2 - 2.2 \times 10^{-10}$ (dynes/cm²)⁻¹ for polyethylene melts.

When the principle stress tenor is rotated counter clockwise (which is

considered positive) through an angle χ , the stress component can be given as:

$$\tau_{12} = \frac{\tau_{p1} - \tau_{p2}}{2} \sin(2\chi) \quad (2.5)$$

and the first normal stress difference as:

$$N_1 = \tau_{11} - \tau_{22} = [\tau_{p1} - \tau_{p2}] \cos(2\chi) . \quad (2.6)$$

From equations (2), (5) and (6), we get

$$\tau_{12} = \frac{\Delta n}{2C} \sin(2\chi) \quad (2.7)$$

and

$$N_1 = \frac{\Delta n}{C} \cos(2\chi) . \quad (2.8)$$

If Δn , C and χ are known then shear stress and the first normal stress difference can be calculated.

An optical setup is used to determine the values of Δn and χ at different points in a given flow. The equation (34) between the fraction of light transmitted, T , isoclinic angle, and the birefringence is given as

$$T = \frac{1}{4} \sin^2\left(\frac{\pi L \Delta}{\lambda}\right) [1 - \cos 4(\chi - \alpha)] \quad (2.9)$$

where α is the polarizer orientation angle.

The sin term is known as the isochromatic term and the cos term is known as the isoclinic term. When this equation is keenly examined, it can be seen

that total extinction can be reached if either the isochromatic or the isoclinic term is zero. When the value of the argument of the isochromatic term is a multiple of π , then extinction of the isochromatic term occurs resulting in a dark band known as the isochromatic band. The isoclinic band occurs when the orientation angle $\alpha = \chi$. Using the method of isoclinics (30) the values of Δn and χ can be found.

The stress Optic Coefficient can then be found by observing the position of the isoclinic and the isochromatic bands of a well characterized flow field of a polymer melt. A plot of shear stress as a function of $\Delta n \sin (2\chi)$ should be a straight line with a slope of $1/2C$.

Polymer Rheology

Kinematics

It has long been realized that Newtonian liquids possess fundamentally different flow properties than polymeric fluids. Several attempts have been made to study the kinematics of polymer melt flow. White (37) was among the earliest to develop a tensor constitutive equation which combined the tensor yield criterion with a non-linear viscoelastic model to represent behavior of concentrated suspensions of small particles in polymeric melts. Yoo and Han (29) have shown qualitative solutions of stress distribution of polymers in extrusion through a converging die by using a Coleman-Noll second order fluid model. Petrie (38) investigated the conditions under which stresses reach steady state values by using an eight constant Oldroyd fluid model.

Hull and Pearson (39) divided the flow field into two distinct regions, elongation dominated and shear dominated, by a streamline, thereby enabling constitutive models to be used. Pearson and Hull could thus model polymer melt rheology reasonably accurately and still retain analytical solutions. Larson (40) and Larson and Khan (20) have made a critical comparison of various constitutive equations for polymer melts in shear and biaxial and uniaxial extensions and found that the superposition integral models were not able to accurately describe reversing deformations, such as elastic recovery or reversing double step strains. Rallison and Hinch (41) have explained the physics involved in the constitutive equation and then tried to correct the undesirable features by looking at micro-structured models like the bead-spring dumbbell model. Samurkas et. al (15) have also studied strong extensional and shearing flow of branched polyethylene and showed that the K-BKZ and Wagner single-integral equations cannot simultaneously describe both strain softening in shear and extreme strain hardening in planar extension. Schunk and Scriven (58) employed combination of the Carreau equation of shear sensitivity with an analogous equation of extension sensitivity. The resultant equation from the combination can be employed to the complex mixed flow in slide coating.

The influence of preshear history, die geometry, and the residence time on the rheology of LCP melt has been shown by Frayer and Huspeni (59). Frayer and Huspeni attributed this dependence to the highly anisotropic nature of the melt. Piliotis et al. (60) have tested various constitutive equation for flow of

shear-thinning viscoelastic fluid through a periodically constricted tube and showed that there was very large increase in the flow resistance with the usage of the modified Phan-Thien-Tanner model.

The different flow behavior can be distinguished by looking at the different elements of the rate of strain tensor. In a two dimensional flow, if the non-diagonal elements of the rate strain tensor are zero, then the flow is termed planar extensional and is highly desirable experimentally due to its shear free nature. However, if the diagonal elements of the rate of strain tensor are zero, then the flow is shearing. Additionally, if only the 1-2 and 2-1 components are non-zero then the flow is termed simple shear. If both the diagonal and non-diagonal elements of the rate of strain tensor are non-zero, then the flow is mixed. Moreover if in any of the cases described above, the flow is spatially dependent then the flow is in nature.

In this study of the flow of polymers through converging channels, all the three regions coexist. The path traced by a particle is known as the stream line. A function describing the stream line is termed as the stream function, which is closely related to the continuity equation. All along the stream line the value of this function is a constant. In rectangular coordinates the velocity components in terms of the stream function can be defined as

$$u_x = -\frac{\partial \Psi}{\partial y} \quad (2.10)$$

$$u_y = \frac{\partial \Psi}{\partial x} \quad (2.11)$$

where \mathbf{u} is the velocity vector and $u_z = 0$. In the case of hyperbolic flow the flow is completely described mathematically if

$$\Psi = \Psi(c) \quad (2.12)$$

where

$$c = \frac{x^2}{\cos^2 \eta} - \frac{y^2}{\sin^2 \eta} \quad (2.13)$$

where η = constant hyperbolic coordinate in elliptical-cylindrical coordinates

since Equation 2.13 is the equation of a hyperbola.

Its essential to find the exact functionality of Eq. 2.14 to find the kinematics.

The velocity field follows from Eq. 2.10 and Eq. 2.11 and is given by

$$u_x = \frac{2y}{\sin^2 \eta} \Psi_c = \frac{\partial x}{\partial t} \quad (2.14)$$

and

$$u_y = \frac{2x}{\cos^2 \eta} \Psi_c = \frac{\partial y}{\partial t} \quad (2.15)$$

where a subscripted c denotes partial differentiation with respect to c . Along a streamline, Ψ is a constant. When Eq. 2.14 and Eq. 2.15 are integrated while subjecting to the initial conditions that $x = x'$ and $y = y'$ when $t = t'$, the displacement equations result:

$$x = x' + \frac{2y}{\sin^2 \eta} \Psi_c s \quad (2.16)$$

and

$$y = y' + \frac{2x}{\cos^2 \eta} \Psi_c s \quad (2.17)$$

where $s = t - t'$. The components of the rate of strain tensor are given by

$$\dot{\gamma}_{xy} = \frac{\partial u_x}{\partial y} + \frac{\partial u_y}{\partial x}. \quad (2.18)$$

$$\begin{aligned} \dot{\gamma}_{xy} = 2\Psi_c \left(\frac{1}{\sin^2 \eta} + \frac{1}{\cos^2 \eta} \right) + \\ 4\Psi_{cc} \left[\left(\frac{x}{\cos^2 \eta} \right)^2 - \left(\frac{y}{\sin^2 \eta} \right)^2 \right] \end{aligned} \quad (2.19)$$

$$\dot{\gamma}_{xx} = 2 \frac{\partial u_x}{\partial x}. \quad (2.20)$$

$$\dot{\gamma}_{yy} = 2 \frac{\partial u_y}{\partial y}. \quad (2.21)$$

$$\dot{\gamma}_{xx} = -\dot{\gamma}_{yy} = \frac{8xy}{\sin^2 \eta \cos^2 \eta} \Psi_{cc}. \quad (2.22)$$

In the special case when $\Psi = A\epsilon$ where A is a constant

$$\dot{\gamma}_{xy} = 2A \left(\frac{1}{\cos^2 \eta} + \frac{1}{\sin^2 \eta} \right) \quad (2.23)$$

and

$$\dot{\gamma}_{xx} - \dot{\gamma}_{yy} = 0. \quad (2.24)$$

This particular flow is referred to as simple shear. If the frame of reference is rotated by 45° then the flow is termed as planar extension.

CHAPTER III

EXPERIMENTAL

The primary aim of this thesis was to independently correlate the kinematics of mixed, heterogenous polymer melt flow in converging channels to the elements of the stress tensor by experiments. A birefringence technique was used to calculate the stress-optic coefficient and study the stress fields. Tracer particle techniques were used to study the kinematics of mixed flow.

Devices capable of generating mixed, heterogenous flow fields and techniques to quantify the results were necessary to complete the work. The flow field was generated in the converging channel section of a specially designed die which was attached to a polymer extruder. The die was fitted with optical windows and placed in an optical train so as to produce birefringence patterns. The die was carefully designed such that extensional flow predominated in the center of the die whereas stress flows were predominate in regions away from the center. In between these regions, mixed flows were present. All the experiments were recorded by a video camera and analyzed manually. The die also contained a slit flow section which was used for measuring the stress optic coefficient. This chapter describes in detail the polymeric materials, experimental equipment, techniques, and procedures used to accomplish the aim of the work.

Material

The polymer resin used was Petrothene (TM) GB 501-010, a Low Pressure Low Density Polyethylene (LPLDPE) and Linear Low Density Polyethylene (LLDPE) obtained from Quantum Chemical Corporation (USI Division). The resin GB 501-010 had a melting point temperature between 100 - 125°C and a specific gravity of 0.9-0.94 (50).

Equipment

A description of the experimental equipment used is presented in this section.

Slit flow Die

The slit flow die was built to the specifications of this project in the Physical Sciences Machine shop at Oklahoma State University and is depicted in Figure 3.1. All parts except the triangular notch in the converging channel were made of stainless steel. The triangular notches were made of brass. The die was carefully designed to produce pure extensional, mixed, and a pure shear flow of molten polymers and to allow observation of flow birefringence and pressure gradient.

The die was a assembly of four stainless steel parts. One of the rectangular strips (38.1 cm x 5 cm x 3.75 cm) contained a 0.254 x 2.54 cm channel. Another plate of the same dimension was used as the upper die half. Window wells 5.0 cm in diameter in the converging region and

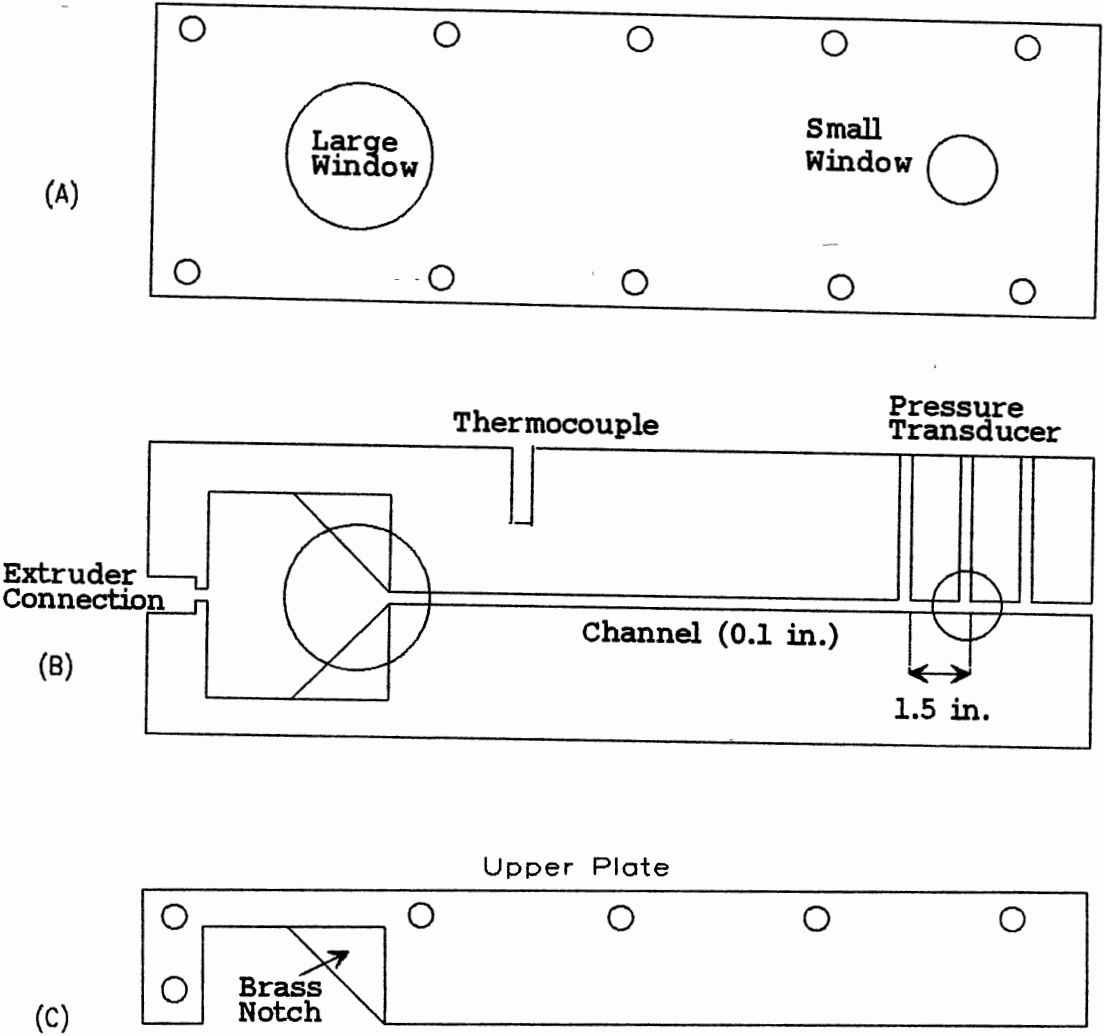


Figure 3.1: Various sections of the Slit Flow Die

2.54 cm in diameter in the slit flow region were drilled. These wells housed the optical windows as is seen in Figure 3.1a. Three pressure wells were drilled on the upper plate as depicted in Figure 3.1b. The pressure wells were designed such that the pressure transducers could be seated flush with the inner edge of the channel and hence did not interfere with the flow. Another port was drilled in the upper plate to act as a temperature well. These two plates were flanked on each side by another pair of plates Figure 3.1, which helped in housing the glass windows. Holes were drilled in the converging and slit flow region to view the flow and also to support the windows. No special efforts were made to seal the clearance between the plates since the leakage was not expected to be very serious under very low flow rates and pressures.

Custom cut, strain free optical windows, made of laboratory grade glass (Ealing Electro-Optics), were mounted in the window wells in each of the plates and were held in place by brackets. The windows were nominally 5 cm and 2.54 cm in diameter at the converging and slit region respectively. Both windows were 1.27 cm thick. The windows were flush seated to prevent any interference with the flow. To cushion the windows from thermal expansion and possible stresses, thin Teflon gasket was placed between each window and the matching bracket. Since the polymer would leak out through the smaller windows when experiments were carried out, additional brackets, made of aluminum, were also placed by brackets. The windows were nominally 5 cm and 2.54 cm in diameter at the converging and slit region respectively. Both windows were 1.27 cm thick. The windows were flush seated to prevent any

interference with the flow. To cushion the windows from thermal expansion and possible stresses, thin Teflon gasket was placed between each window and the matching bracket. Since the polymer would leak out through the smaller windows when experiments were carried out, additional brackets, made of aluminum, were also provided. All the plates were clamped together with eight bolts on top and another set of eight bolts along the sides.

During operation, the assembled slit flow die was mounted to a Killion polymer extruder with a 1 in. screw (model number KLB-100). The die was heated with electrical heating insulated fiberglass tapes (rated at 240 VAC). These heating tapes and the die were insulated for high temperatures with ceramic wool insulations. A combined temperature and pressure transducer (TPT 432A, Dynisco Inc.) was mounted in the middle of the three pressure ports to measure the temperature and pressure of the polymer melt simultaneously. Two other pressure transducers (PT422A Dynisco) occupied the other ports. A feedback control thermocouple was seated in the temperature well. The heating of the extruder die, and the feedback control, all were controlled from the extruder.

Optical and Video Setup. The optical train consisted of a light source, collimating lens, filter, polarizer, sample, and the analyzer. The order of arrangement of the different elements of the optical train is shown in Figure (3.2).

The light source was a 150 W fiber optic source (Ealing Electro-Optics) with a fiber optic bundle of 0.635 cm diameter and 61 cm in length. All the elements

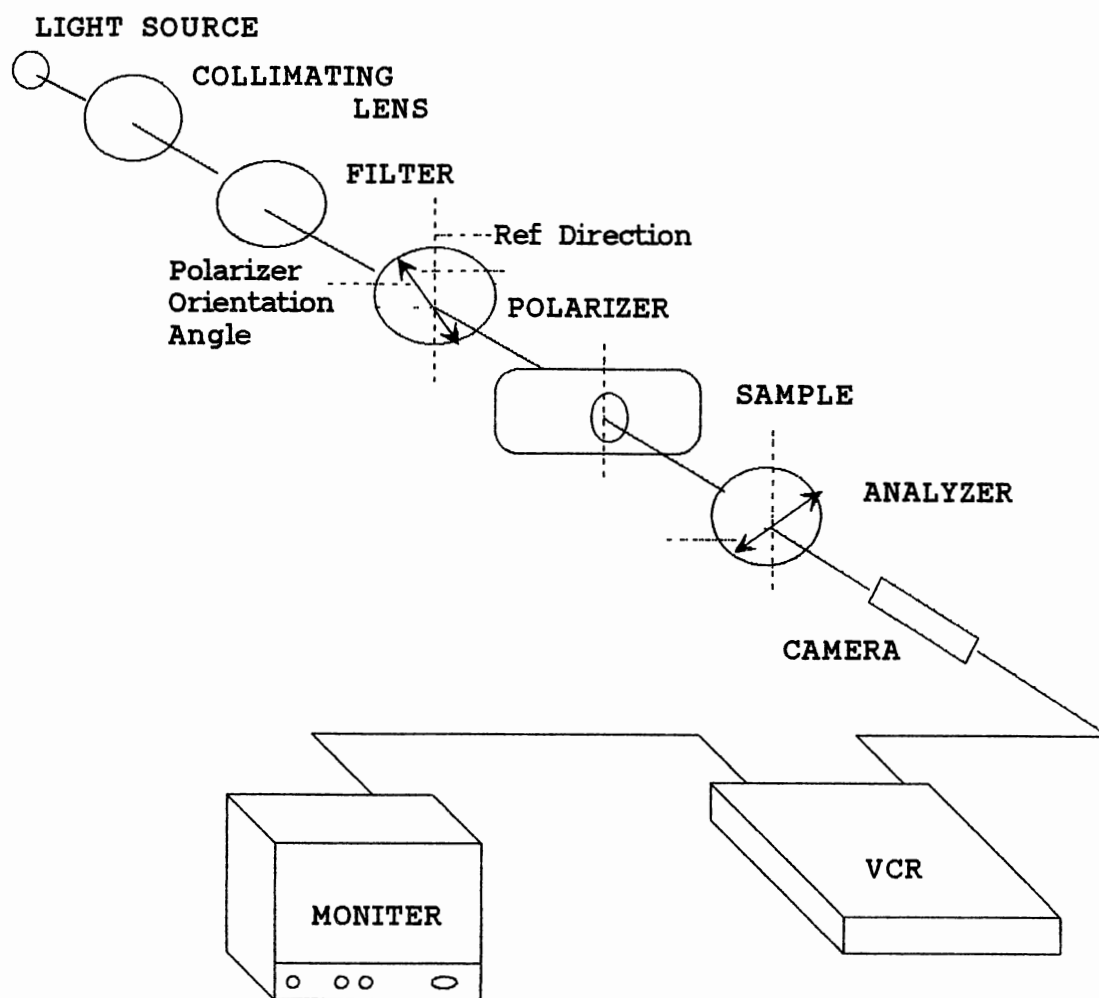


Figure 3.2: Optic and Video Setup

of the optical train were mounted on an aluminum optical rail in their respective holders and held in position by a clamp. The collimating lens was used to direct parallel beams of light through the sample (die). The collimating lens was 75 mm in diameter and had a focal length of 150 mm. The light filter had maximum transmission at 488 nm (blue) with a bandwidth of 7.2 nm and a maximum transmission of 45%. The polarizer and the analyzer were 101.6 mm in diameter. The polarizer and the analyzer were manually rotated in unison.

The video setup consisted of a video camera, monitor, and a VCR. The video camera was a black & white Javeline NEW VI CHIP CCD. An additional set of lenses known as a closeup kit were used to obtain a better magnification of the slit flow region. The monitor was a black & white Javelin (model number BWM12). The monitor was connected to a RCA VCR (model number VR520) which had many additional functions such as frame by frame advance, control speed record and playback etc.

Technique and Procedure

Rheological Data

Data needed for correlating the flow kinematics and stress fields were obtained independently of each other. A birefringence technique was used to calculate the stress-optic coefficients and tracer particle technique to study kinematics.

To start an experiment, the extruder and the die were heated to the desired temperature with the help of a feed back controller. A picture and description

of the die can be found in Appendix E. The heating was carried out by setting the temperature in the different zones of the extruder so as to create a constant temperature gradient. For example: when the die was set at 150 °C, Zone 1 of the extruder was set to 140 °C, Zone 2 at 150 °C, and Zone 3 at 160 °C. The extruder was allowed to heat until thermal equilibrium was reached. The time taken to reach this thermal equilibrium was around 2 hours. The optic train is setup as shown in Figure 3.2, such that the light would pass through the desired window. All the optical components were maintained at constant height above the stand. After the polymer had melted, the fiber optic light source was turned on. To obtain reproducible results, it was essential to focus the camera on the center of the flow. In order to focus the camera on the center of the flow, the camera was focused on the front edge of the front window. The camera was then moved forward until the back edge of the rear window was in focus. An average of the two camera positions was used during data collection.

The polarizer and the analyzer were held perpendicular to each other by setting them to 0° and 90° respectively. However for the sake of convenience and to avoid confusion the analyzer was "flipped" 90° so that both the polarizer and the analyzer would be perpendicular when set to 0°. The extruder motor speed dial was set to the desired RPM and the flow videotaped. Care was taken to record the birefringence from the time of inception of flow to check the order of the central band. Once steady state was attained further recordings were made by turning the polarizer and the analyzer in unison, counter

clockwise, through steps of 5° . The analyzer was removed from the optic train when recording the path of the tracer particles. This eliminated the interference of the birefringence bands during the analysis. The inherent particles in the polymer were satisfactory as tracer particles.

The video tapes were analyzed as follows to determine the streamline:

- (1) a transparency was held up on to the screen;
- (2) the video cassette recorder and the monitor were turned on;
- (3) particles which were clearly focused were chosen to ensure that only the center of the flow was being visualized;
- (4) the position of each particle was marked on the transparency at time intervals of one second (every 30th frame);
- (5) the horizontal and the vertical distance of the particle from the center of the slit die entrance to each particle position, was manually measured.

The procedure was repeated for many such tracer particles at each flow rate and temperature in order to get representative sets of streamlines. The path traced by these particles were then plotted and fit to Equation 2.15.

Stress fields were developed using the method of Isoclinics (30). The shear stress and the first normal stress difference were calculated from the isoclinic angle, birefringence, and the stress-optic coefficient by use of Equation 2.7 and Equation 2.8. Plots showing the shear stress fields were then prepared.

Stress Optic Coefficient

The stress optic coefficients were also measured using the Method of Isoclinics (30). In this case the flow of polymer melt through the slit portion of the die was video taped as explained above. Care was taken to note the order of the central band. The distance of the inner edge of the isoclinic band from the center of the slit was then measured. The pressure gradient along the slit region at a distance far away from the inlet, where the flow had attained steady state, was measured using three pressure transducers. A plot of this pressure with respect to distance from the die inlet was then made. The plot should be a straight line in steady fully developed flow, from which the pressure gradient could be determined. With the knowledge of the pressure gradient and the distance of the isoclinic bands from the centerline, the shear stress could be calculated at each isoclinic position. From a knowledge of birefringence and the isoclinic angle, a plot of shear stress on the ordinate versus the product of birefringence and sine value of twice the isoclinic angle is made to fit a straight line. The inverse of the slope is twice the stress optic coefficient. The stress optic coefficient was then used in calculating the shear stress and the first normal stress difference in the converging section.

CHAPTER IV

RESULTS AND DISCUSSIONS

The results of the rheo-optic analysis of a polymer melt in heterogenous, mixed flow kinematics are presented in this chapter.

Stress Optic Coefficients

The method of Isoclinics (30) was used to measure the stress optic coefficient (SOC). The SOC is calculated from the knowledge of the birefringence, the isoclinic angle, and the shear stress.

The birefringence and the isoclinic angle were obtained in the slit flow by rotating the polarizer and the analyzer, counter clockwise, in unison while in the crossed position. In the initial state the polarizer was oriented parallel to the direction of flow whereas the analyzer was oriented perpendicular to the flow direction. When monochromatic light was passed through this sample, alternating dark and bright bands appeared. Bands originated from the upper and lower walls of the slit, and approached the center. The first band originating from the walls is known as the zeroth order band. The bands following the zeroth order band are subsequently given the order of first, second, third, etc. The bands which occur when $(L\Delta/\lambda)$ equals a whole number are called isochromatics. An example of a birefringence pattern is seen

in Figure 4.1 for LLDPE at a temperature of 150 °C, RPM = 7.0, and $\alpha = 0$.

Figure 4.1 shows the isochromatic bands as seen on the video monitor. The bright region, with bands, is the area of interest. The outer dark region represent the front wall of the die. The order of bands is assigned from the center towards the wall, in an ascending fashion. The central band is the zeroth order band and is flanked on either sides by the first order, followed by second order, third order etc..

As the polarizer and the analyzer were rotated a thick, dark band appeared at the top of the screen, ie. from the upper edge, and overlapped the isochromatic bands. This thick band is known as the isoclinic band, and appears when ever χ , the isoclinic angle, equals α . An example of a birefringence pattern with an isoclinic and isochromatic bands is seen in Figure 4.2. The isoclinic band shown in Figure 4.2 was obtained by rotating the polarizer and the analyzer, in the counter clockwise direction, through an angle of 30° at the same flow conditions and temperature as that of Figure 4.1. The only difference between Figure 4.1 and Figure 4.2 is the presence of isoclinic band.

In order to obtain the SOC, a well characterized shearing flow and a knowledge of the shearing forces acting at different points in the flow was essential. A steady shearing flow was obtained in the slit die (as described earlier) and the stresses calculated at various points from the well known solution of the equations of motion:

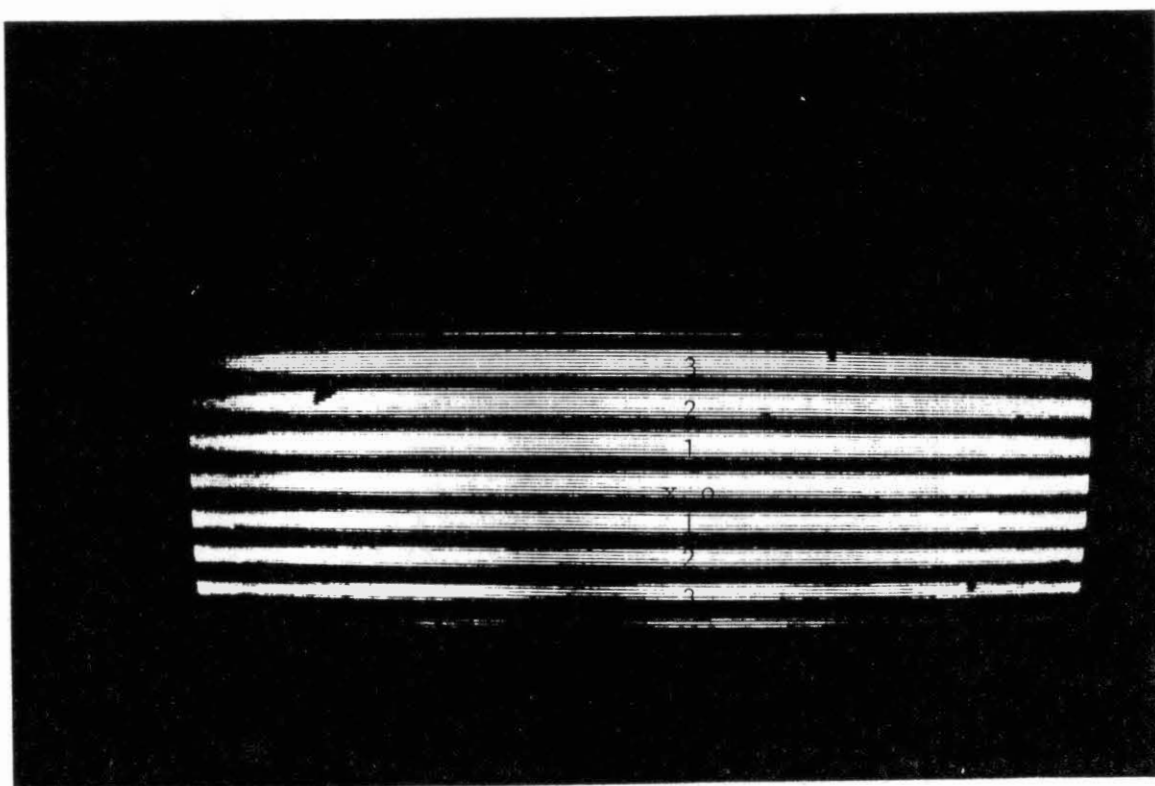


Figure 4.1: Slit Flow Birefringence Pattern at 150 °C and $\alpha = 0$

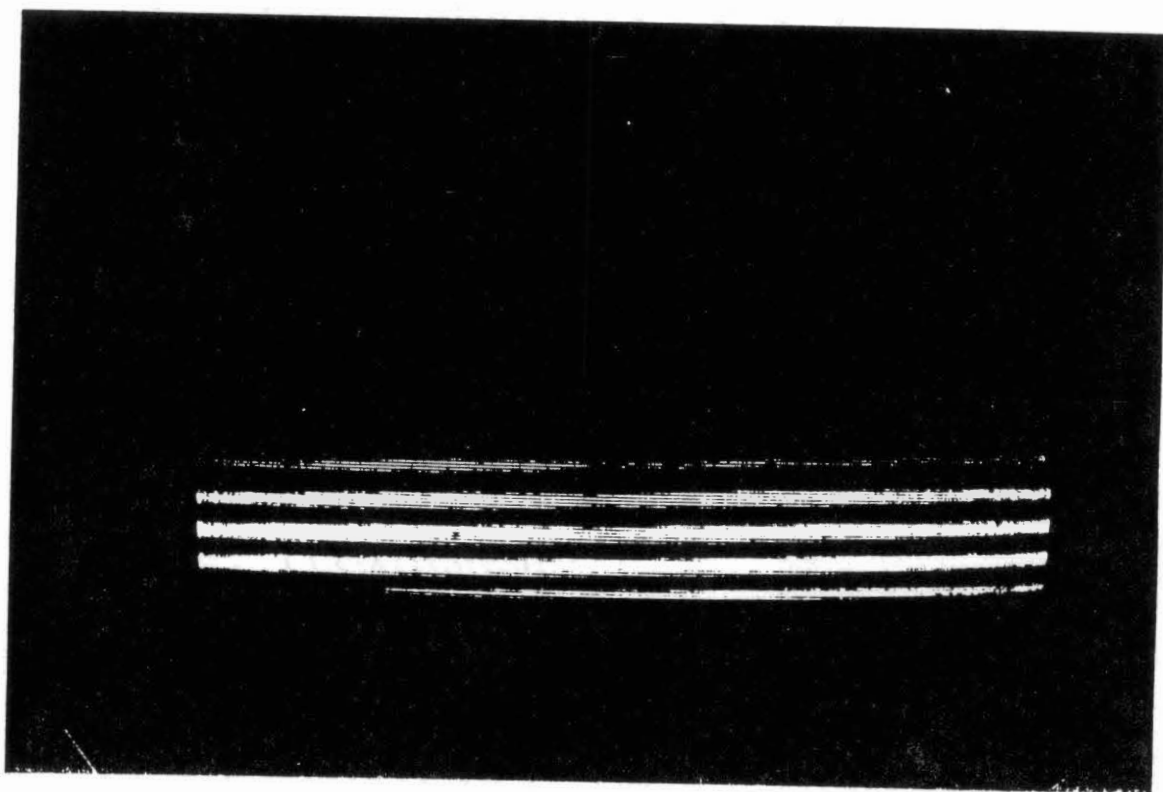


Figure 4.2: Slit Flow Birefringence Pattern at 150 °C and $\alpha = 30$

$$\tau_{xy} = y \frac{\partial P}{\partial x} = \tau_w \frac{y}{b} \quad (4.1)$$

where $\partial P / \partial x$ = pressure gradient

τ_w = wall shear stress and

b = half height of the slit.

For a given χ , the distance of the isoclinic band from the center of the flow was measured and the stress calculated from the knowledge of the pressure gradient. A plot of the pressure indicated by the pressure transducer vs distance from the die inlet was made. A plot of pressure as a function of y , for a temperature of 150 °C and RPM rate of 9, is shown in Figure 4.3. The plot appears to be linear.

In the converging section, Figure 4.4, isochromatics, are seen to be parallel to the die wall, at a distance, approximately one to two times that of the die height, beyond the die entry, indicating that the stresses had become independent of flow direction at that point. Since the window in slit flow section of the die was at a distance of about 40 times the die height, it can be concluded that the flow at the windows was fully developed. The above conclusion is further supported by the linear behavior of the pressure data as shown in Figure 4.3. Thus it can be further concluded that all the data in the slit flow section were taken in a fully developed shearing flow.

The birefringence is a continuous function from the center of the slit to the edge. For a particular isochromatic band, the birefringence is given by:

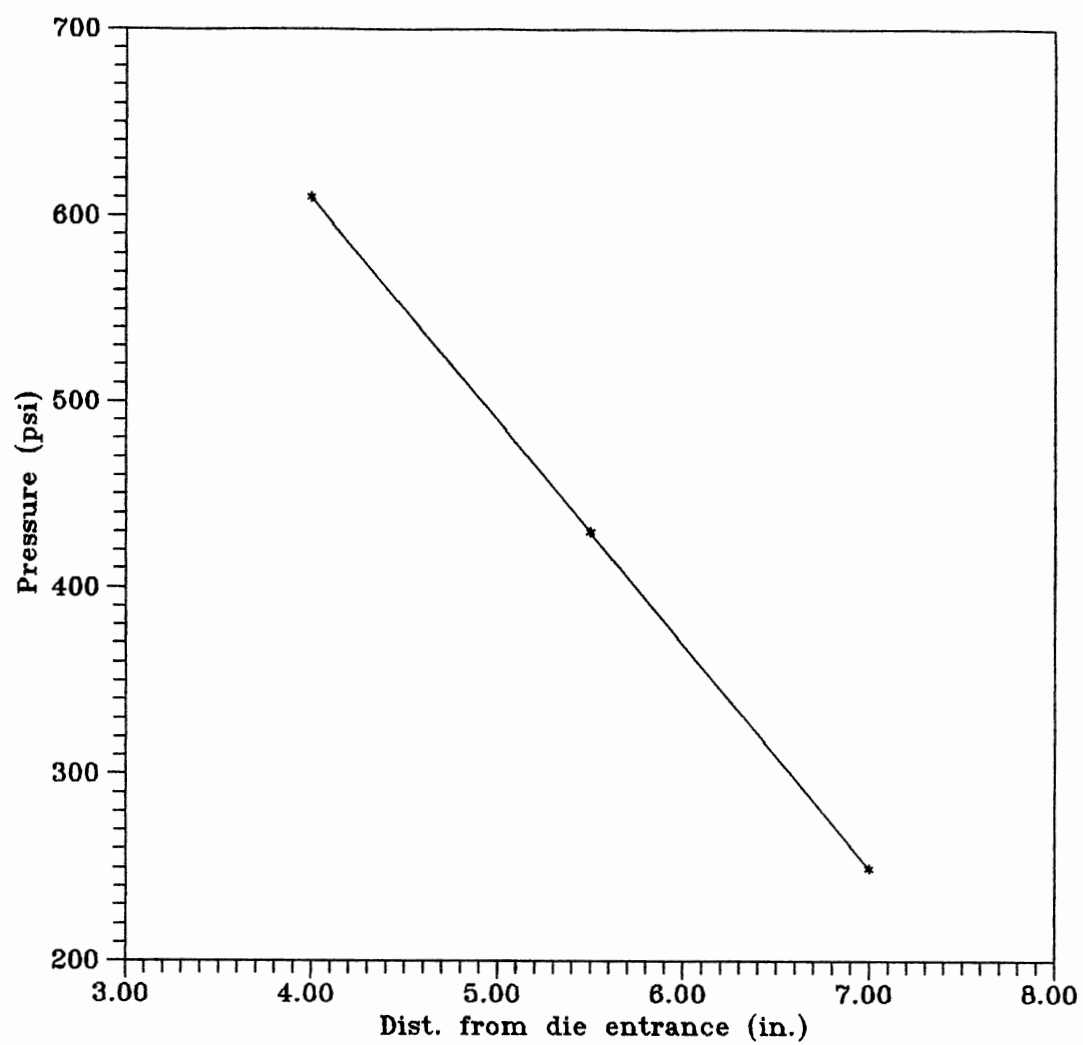


Figure 4.3: Steady State Pressure Gradient at 150 °C and 9 RPM

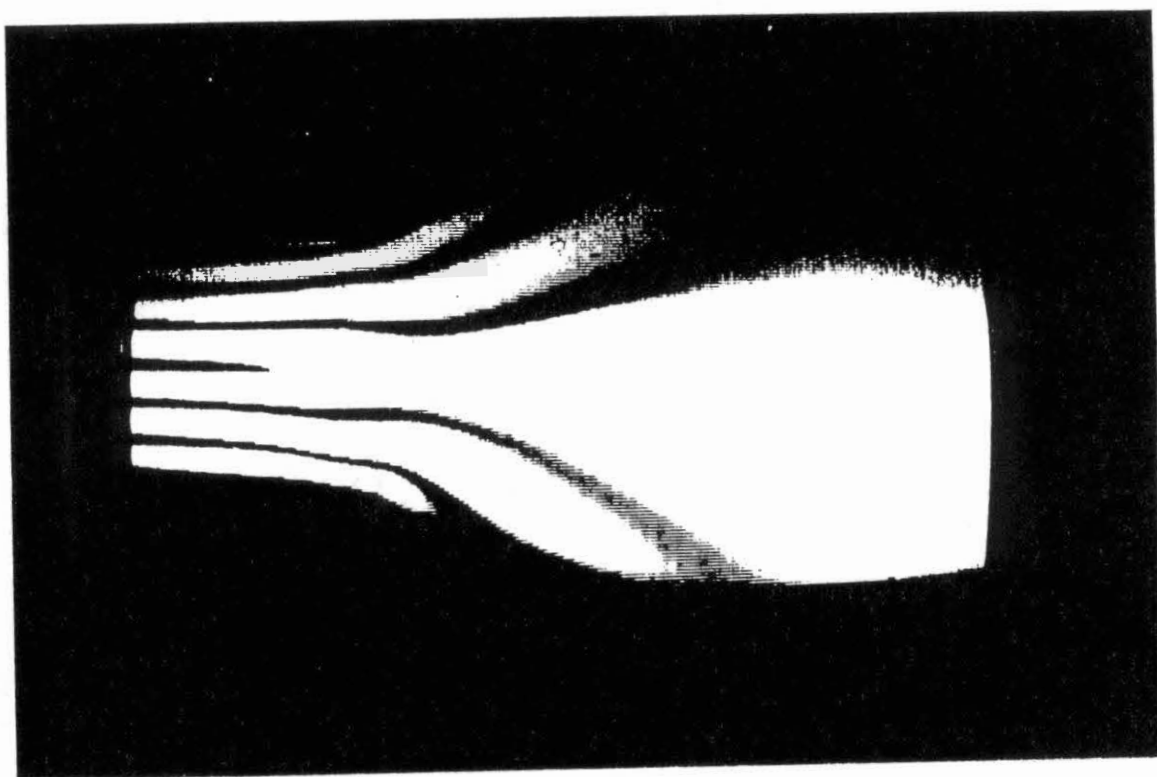


Figure 4.4: Birefringence Pattern in the Converging Section at 150 °C, RPM = 7, and $\alpha = 0$

$$\Delta n = \frac{m\lambda}{L} \quad (4.2)$$

where m = order of the band

λ = wavelength of light used

L = length of the neutral direction.

The birefringence of points intermediate to the isochromatics were found by linear interpolation.

A plot of τ_{12} on the ordinate and $\Delta n/2 \sin 2\chi$ on the abscissa was then made to verify that the equation:

$$\tau_{12} = \frac{\Delta n}{2C} \sin(2\chi) \quad (4.3)$$

where χ is the isoclinic angle, was satisfied. The graph obtained is shown in Figure 4.5 for a melt temperature of 150 °C. A linear least square fit was applied to the data. All the data points fall on or near the line with only a little scatter, thereby indicating that the linear stress optic relationship holds. The best fit line passes very closely to the origin, giving evidence of the accuracy of the method of isoclinics (30). The inverse of the slope of this line gives the stress optic coefficient C . The stress optic coefficient for the example case shown in the Figure 4.5 was found to be $1.4 \times 10^{-10} \text{ (dynes/cm}^2\text{)}^{-1}$.

The stress optic coefficient of LLDPE was determined for a temperature range of 140 °C (413 K) to 185 °C (458K). All values compared favorably with data from the literature (31, 32, 33). The variation of C with temperature for LLDPE and the literature values are shown in Table 3.

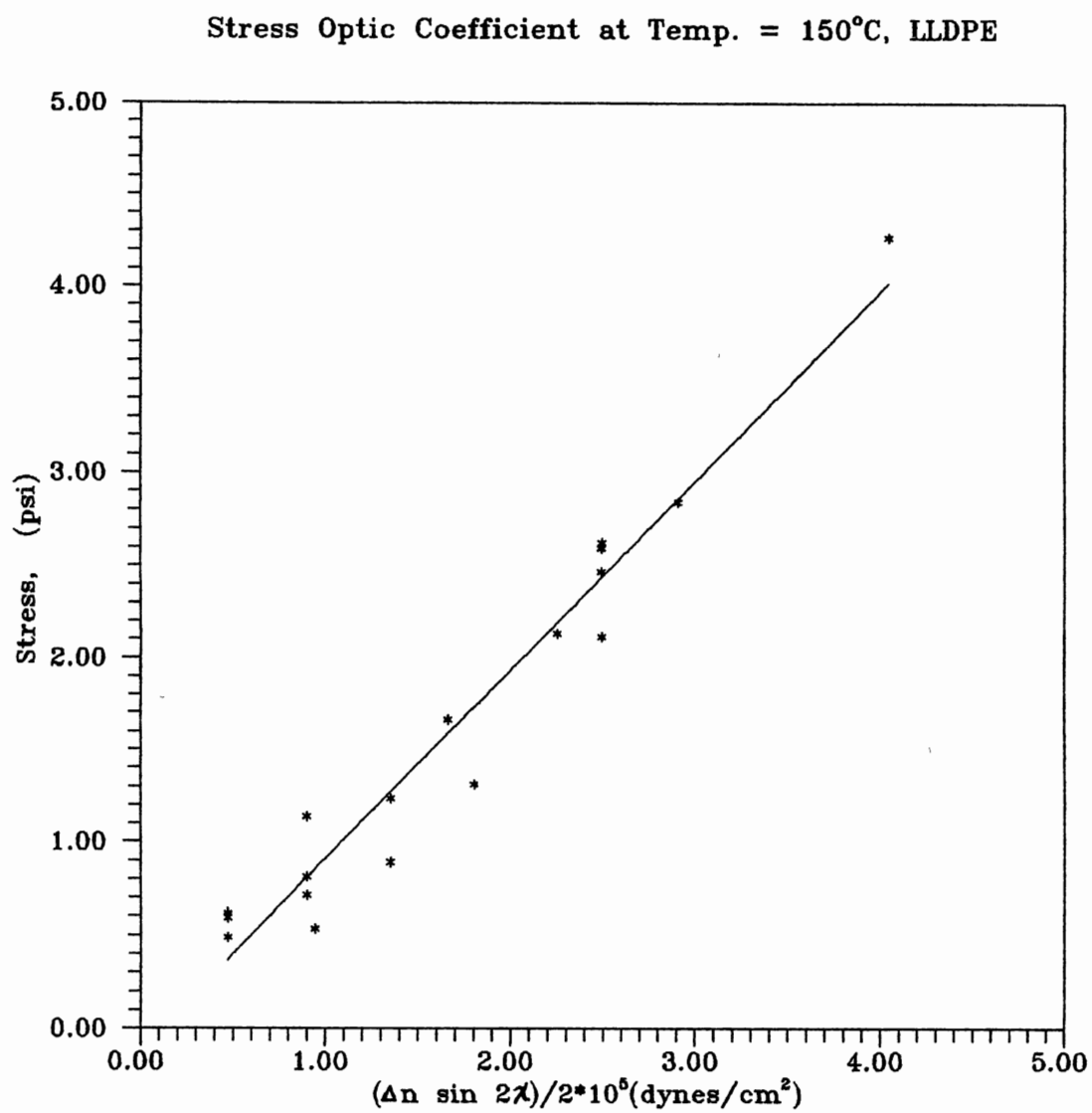


Figure 4.5: Calibration of C at 150 °C

TABLE 4.1
VARIATION OF STRESS OPTIC COEFFICIENT
WITH TEMPERATURE

Temperature (K)	SOC (dynes/cm ²) ⁻¹
413	1.5×10^{-10}
423	1.4×10^{-10}
443	1.2×10^{-10}
458	1.1×10^{-10}
Literature (31, 32, 33)	$1.2 - 2.2 \times 10^{-10}$

The first normal stress difference was then obtained from Equation 4.4, given as:

$$N1 = \tau_{xx} - \tau_{yy} = \frac{\Delta n}{C} \cos(2\chi) \quad (4.4)$$

by using the value of C obtained earlier. A plot of Equation 4.4 is shown in Figure 4.6. The plot is a straight line. This leads to the conclusion that in a slit flow die, the shear stress and the first normal stress difference are related in a directly proportional fashion. The results obtained are consistent with those already found in the literature (27). The proportionality of the shear stress and first normal stress difference is evident from Figure 4.7.

Attempts to apply molecular models to treat birefringence behavior have been made by Kuhn et. al (48). The expression for the stress optic coefficient resulting from this work is given by:

$$C = \frac{2\pi}{45} \frac{(n^2+2)^2}{n} \frac{\alpha_1 - \alpha_2}{kT} \quad (4.5)$$

where k = Boltzman constant
 $\alpha_1 - \alpha_2$ = difference in polarizability
 n = average refractive index
 T = absolute temperature.

This equation leads to the expectation that the stress optic coefficient is inversely proportional to the temperature. Janeschitz-Kriegl (35) has shown that the inverse proportionality is not generally true. To account for the deviation, Treloar (47) suggested a different form to represent the optical anisotropy which

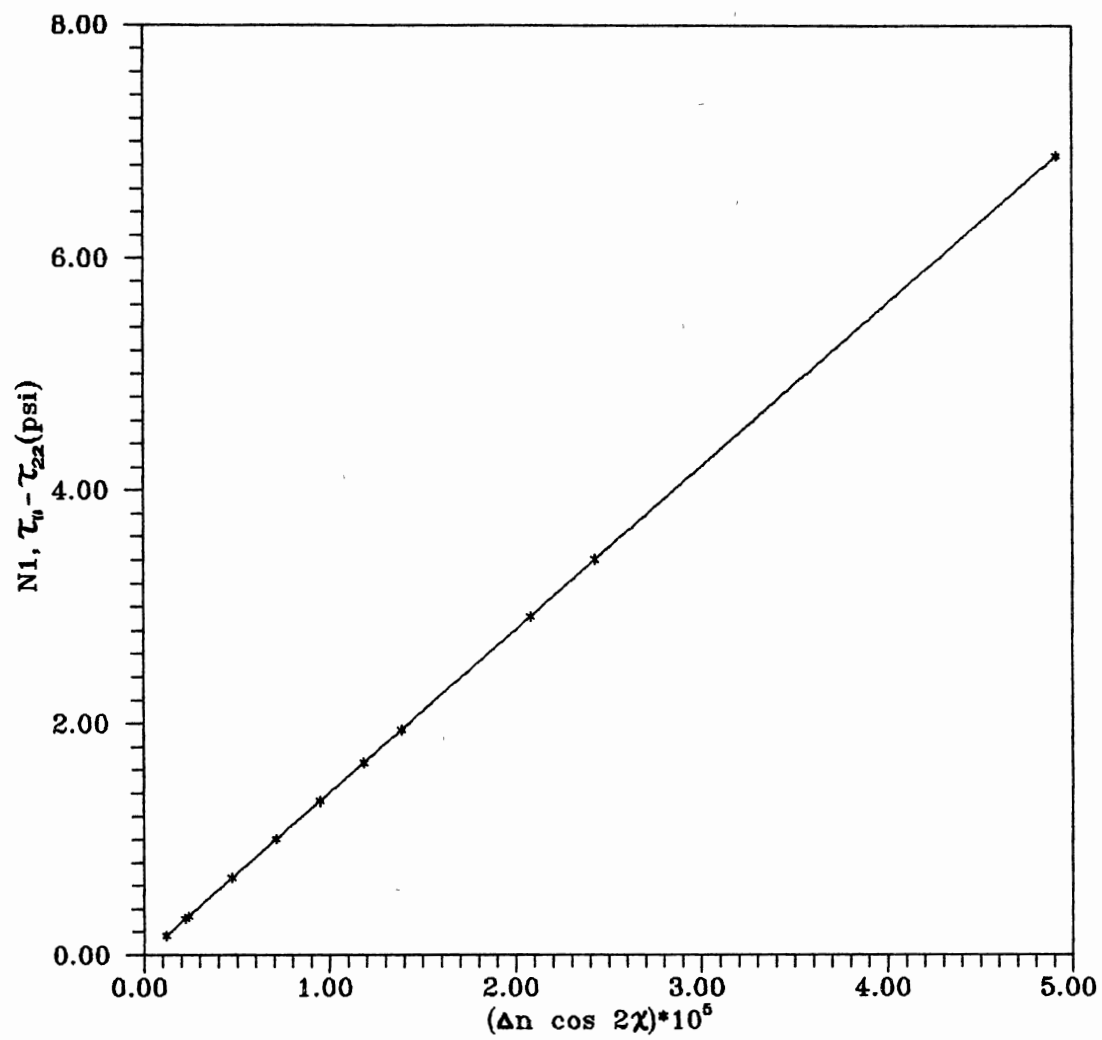


Figure 4.6: First Normal Stress Difference at 150 °C

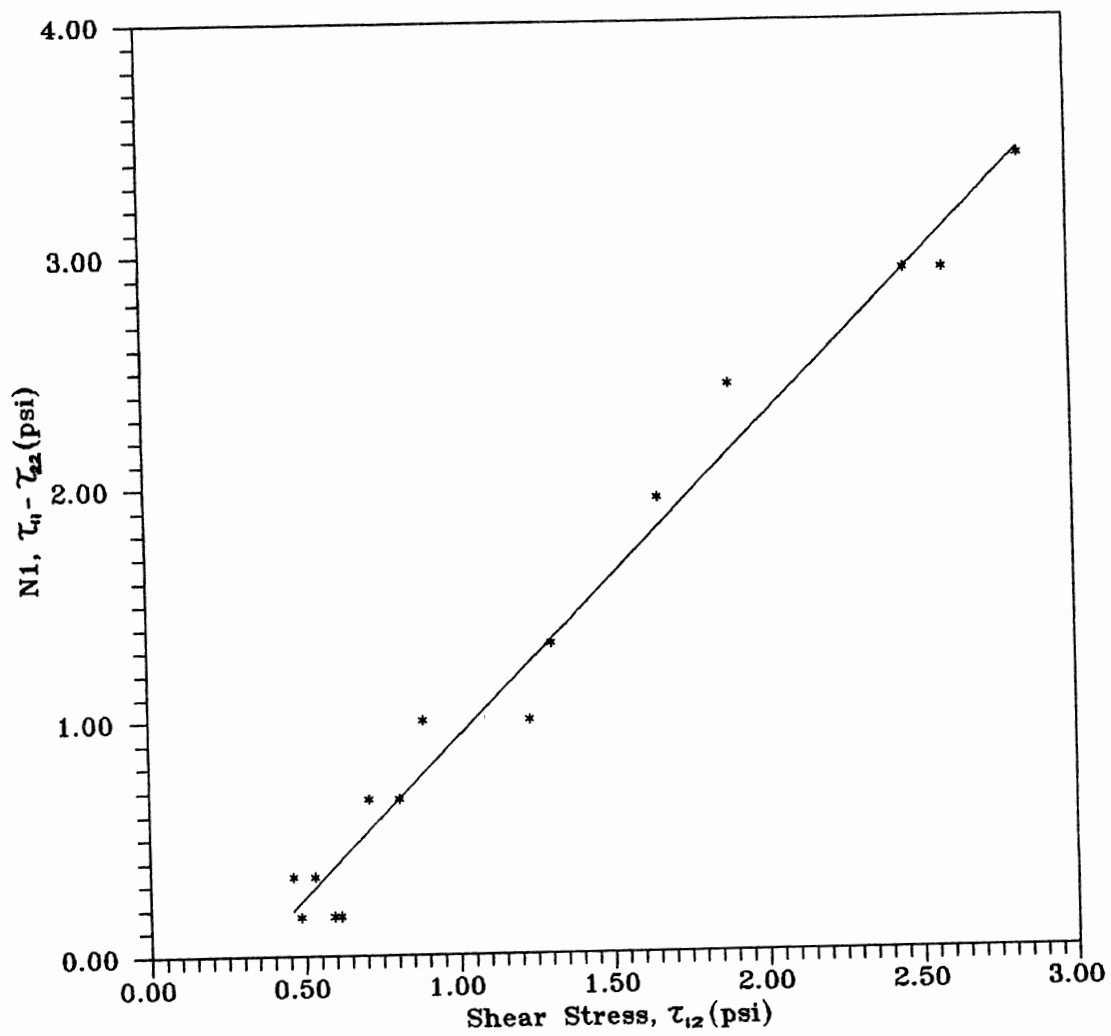


Figure 4.7: Shear Stress as a Function of First Normal Stress Difference

is due to the difference in polarizability:

$$\alpha_1 - \alpha_2 = A e^{\frac{E}{RT}} \quad (4.6)$$

where E is the activation energy

A is a constant

R is universal gas constant.

T is temperature

A combination of Equations 4.4 and Equation 4.5 leads to

$$C = \frac{2\pi}{45} \frac{(n^2 + 2)^2}{n} \frac{A e^{E/RT}}{kT} \quad (4.7)$$

Treloar (47) demonstrated that for various polymer systems a plot of the natural logarithm of the product CT as a function of 1/T is a straight line. Figure 4.8 illustrates this verification for the LLDPE data of this study. Thus it can be concluded that the stress optic coefficient obtained were sufficiently accurate for further use.

Rheology

Converging Section

In this section, results of the converging section study are presented for the example case of LLDPE at 150°C and 7 RPM. All the data related to the study of converging section appears in Appendix C. The birefringence technique, was employed to determine the stresses acting at different points in this region, from the knowledge of the stress optic coefficient, C,

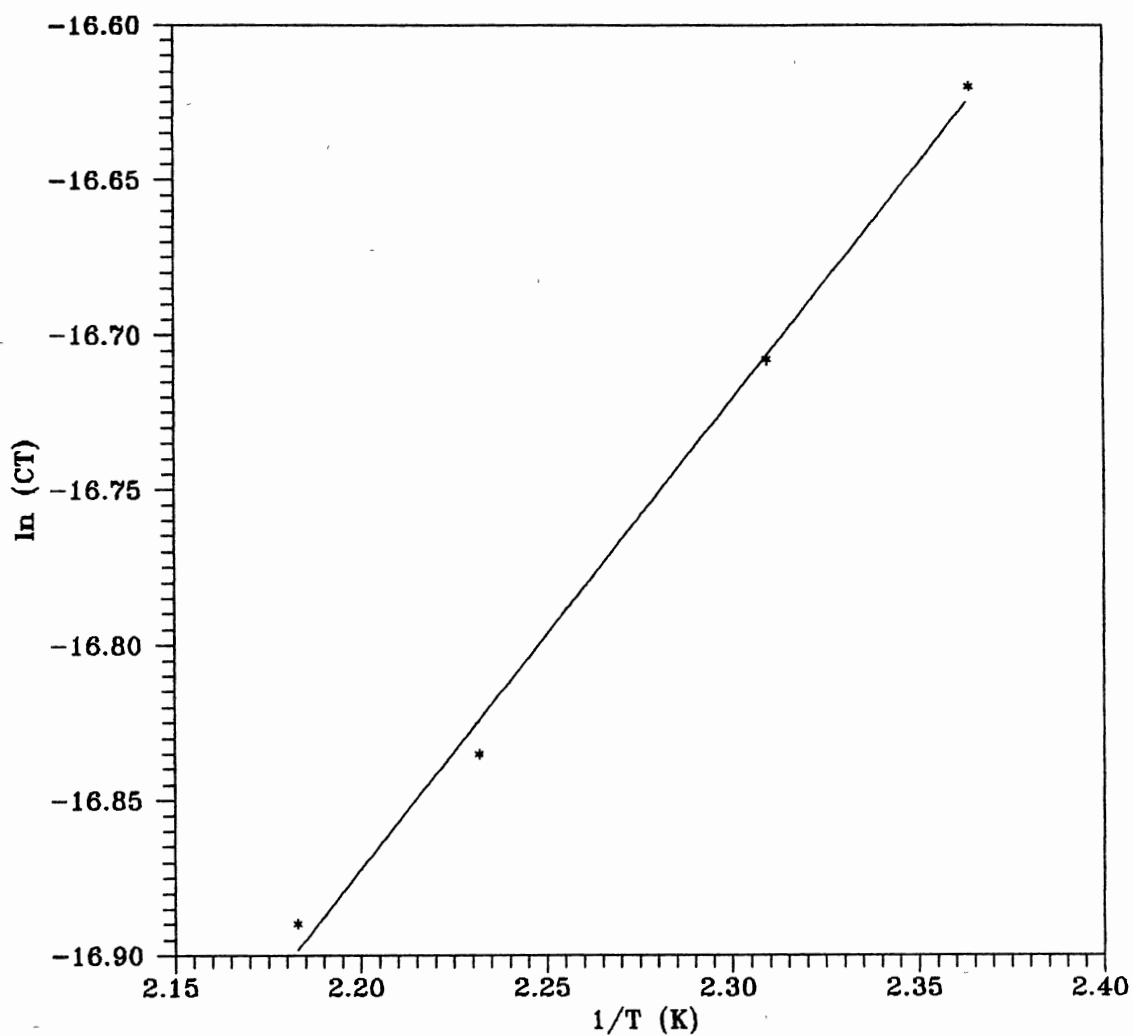


Figure 4.8: Natural Log of CT as a Function of Inverse Temperature

polymer and temperature. A tracer particle technique was used to analyze the kinematics of the converging section of the die. Care was taken to be accurate in taking data points as they are susceptible to manual misjudgment. A suitable coordinate system was defined and stress fields quantified.

A typical birefringence pattern is shown in Figure 4.4. Three bands are seen on either side of the center of the slit entrance. The bands near the entrance are the isochromatic bands. The broad bands away from the entrance are the isoclinics. Both of these bands have been marked distinctly in Figure 4.4. At this point it is essential to note that care must be taken to distinguish the isoclinic bands from the isochromatic bands. The isoclinics and the isochromatics can be distinctly distinguished by employing a quarter wave plate.

The locus of points connecting regions of the same stress were then plotted as shown in Figure 4.9. From the Figure 4.9, it can be seen that: (1) the shear stress goes through a minimum at the center line with maximum stress occurring at the die walls, (2) the shear stress profiles are parallel at the entrance of the slit die, (3) the shear stress decreases with increasing distance from the slit die entrance. Thus it can be concluded that the shear stress emanating at the walls moves towards the center of the flow. This is reasonable from the well known equation of continuity that the shear stress is maximum at the walls and zero at the center of a flow between two parallel plates.

The first normal stress difference was then plotted as shown in Figure 4.10.

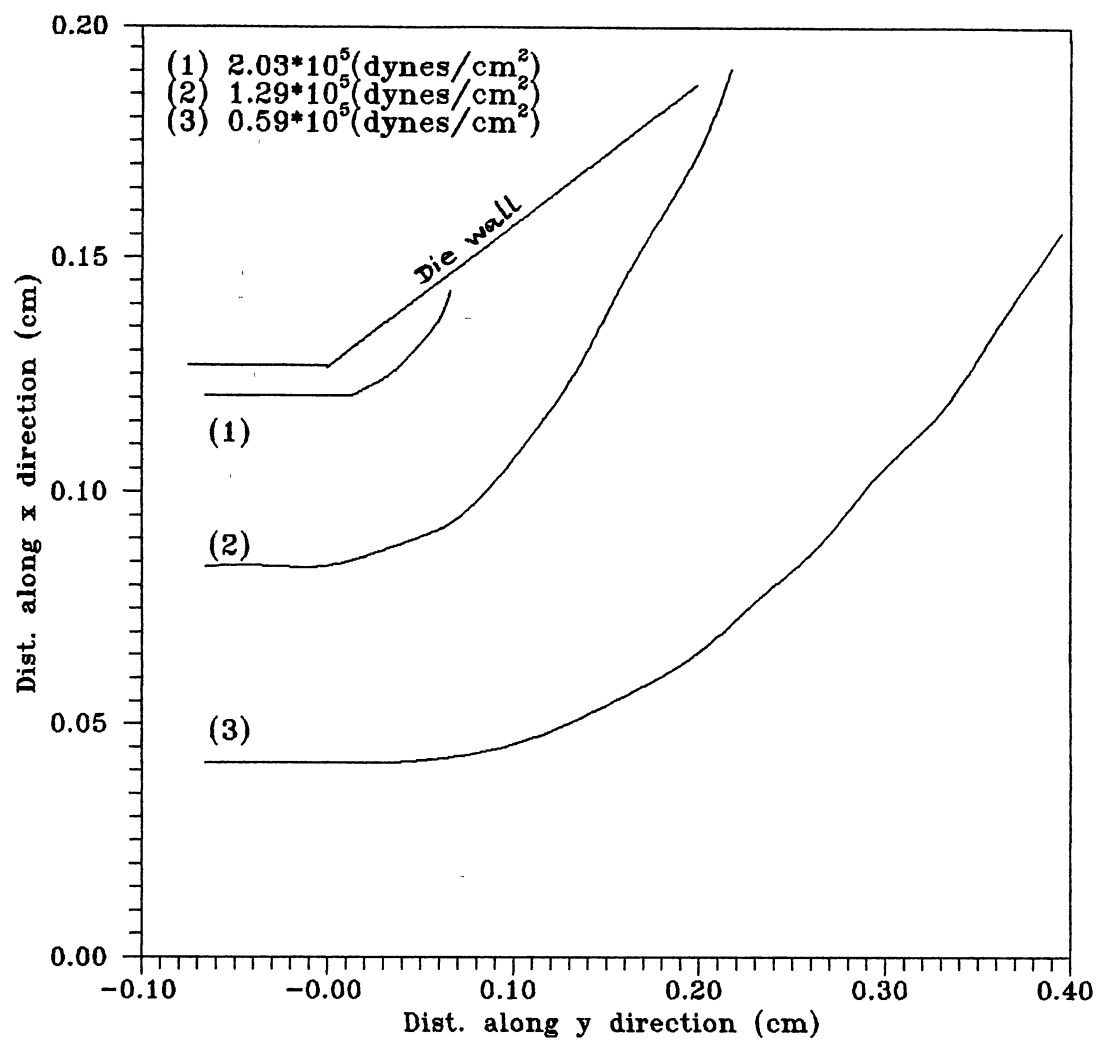


Figure 4.9: Stress Field Distribution of LLDPE at 150 °C, RPM = 7

From Figure 4.10, it can be seen that the first normal stress difference goes from a minimum at the wall to a maximum at the center passing thr. Thus it can be concluded that the shear stress emanating at the walls moves towards the center of the flow. This is reasonable from the well known equation of continuity that the shear stress is maximum at the walls and zero at the center of a flow between two parallel plates.

The first normal stress difference was then plotted as shown in Figure 4.10. From Figure 4.10, it can be seen that the first normal stress difference goes from a minimum at the wall to a maximum at the center passing through a region of zero first normal stress difference. This observation is expected and can be explained thus: the velocity vector can be resolved into two components, the x directed velocity and the y directed velocity. Near the walls the x component dominates, whereas near the center the y component dominates. At a point in between both components contribute equally, resulting in a cancellation. Thus the results obtained are reasonable. Also the result thus obtained is consistent with various other studies (27).

The ability of the elliptical-cylindrical coordinates (51), Figure 4.11, to describe the streamlines in the converging section was demonstrated. Figure 4.11 depicts the axis of the elliptical-cylindrical coordinates. Any point in space is uniquely represented in this coordinate system by the intersection of a constant ellipse, a constant hyperbola, and a value of z . The coordinate surfaces are elliptical cylinders ($\eta = \text{constant}$), hyperbolic cylinders ($\psi = \text{constant}$), and parallel planes ($z = \text{constant}$).

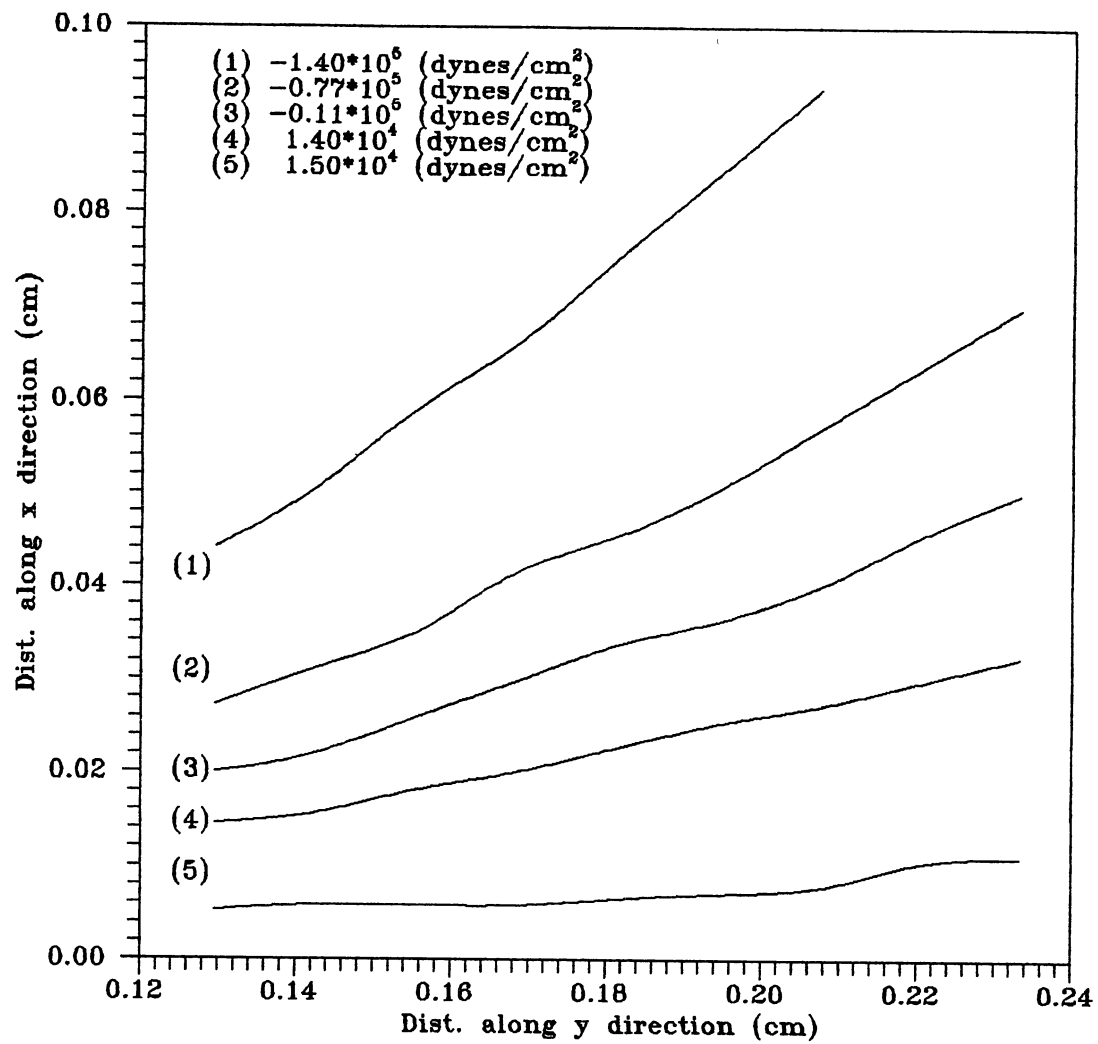


Figure 4.10: First Normal Stress Difference in the Converging Section
at 150 °C, RPM = 7

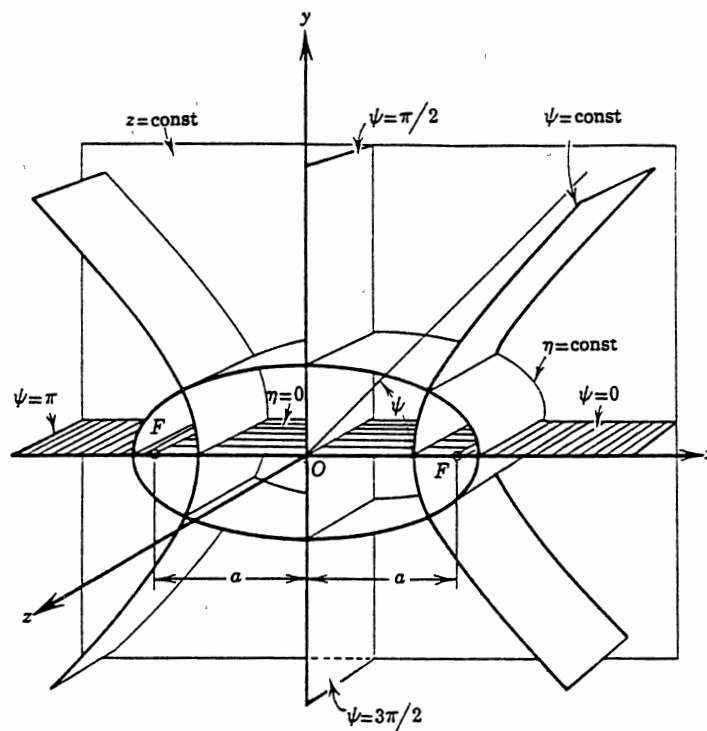


Figure 4.11: Elliptical-Cylindrical Coordinates

The plot in Figure 4.12 depicts the path of different tracer particles. The lateral and the vertical distances were measured from the slit entrance point. The positions of the tracer particles at a given instance are indicated by the data points. The solid lines represent ideal elliptical hyperbolic paths.

From Figure 4.12, the following observations and conclusions can be made:

- (1) the streamlines do not intersect, as required by the law of continuity, hence the streamlines are good representation of the path traced by the particles; (2) as the particle approaches the slit die entrance the x-directed velocity becomes small, concluding that the velocity is greatly contributed by the y-directed component of the velocity, which is expected for the geometry of the die used;
- (3) from the distance between the points on the graph for a particular streamline, it can be concluded that the y-directed velocity and the overall velocity increases as the particle approaches the slit entrance. Also the particles move with a higher velocity at the center of the flow than near the walls, which must be true for the continuity equation to hold; (4) the profile of the streamline becomes more flat as the center is approached, indicating that the y component of the velocity increases much more rapidly than the x component of the velocity; (5) at points away from the center, towards the wall, both the x and the y component contribute equally towards the velocity vector;
- (6) when the streamlines adjacent nearer to the wall are carefully analyzed, it is seen that large velocity deviations occur within a small distance from the wall towards the center, leading to a plug flow like profile as is often seen in polymer melts in polymer melts; (7) the experimental data and the profiles fit to Equation

Streamlines at 150 °C and 7 RPM, LLDPE

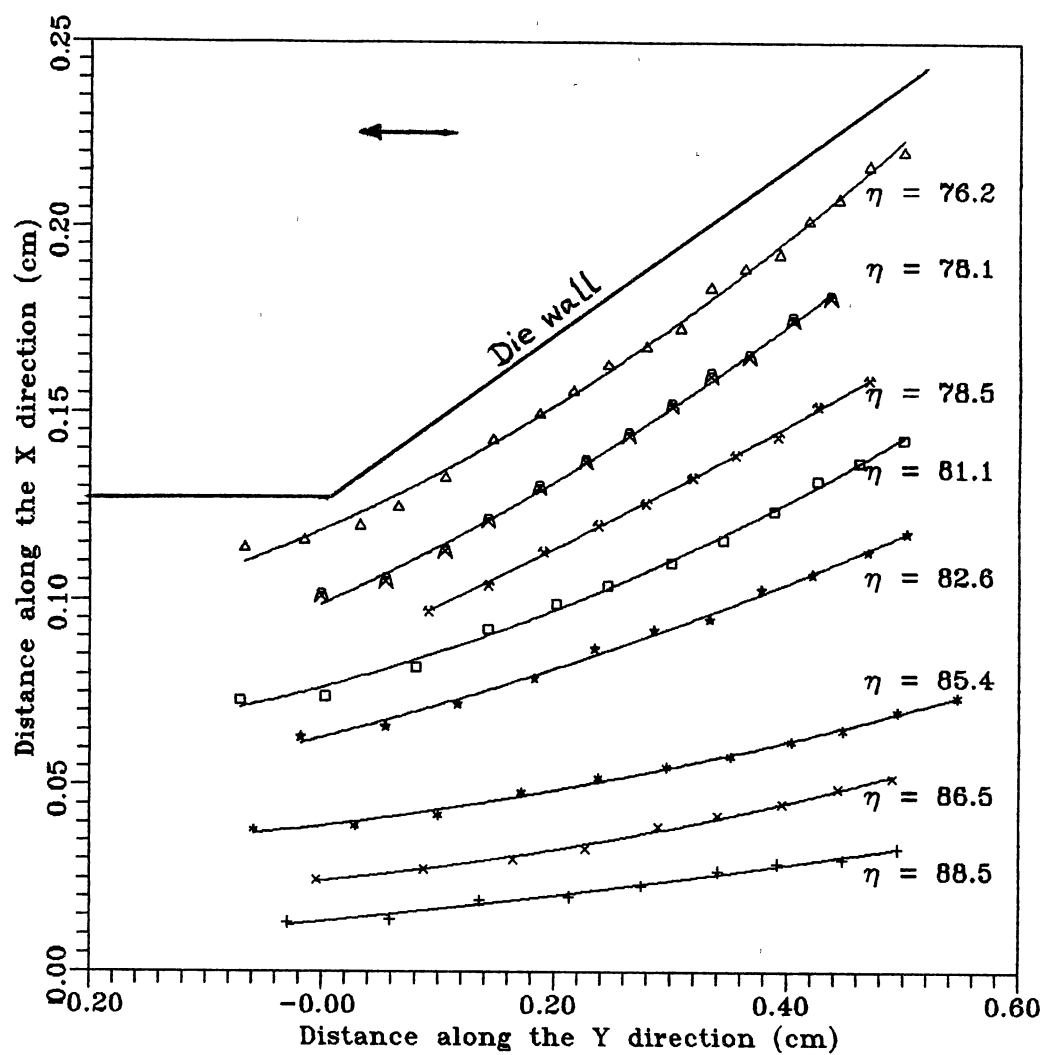


Figure 4.12: Tracer Particle Analysis at 150 °C, RPM = 7

2.15 are in good approximation of each other. The good approximation is acceptable due to their reproducibility characteristic; (8) since no distortion of the tracer particle profile was seen it can be concluded that no vortices were found to occur.

At each position of a particular tracer particle along a given streamline, values of the constant, c , were calculated and then averaged. The value of Ψ_c was then calculated using the method of least squares for both x and y coordinates at a particular point based on Eq. 2.18, and Eq. 2.19. The values of Ψ_c based on these coordinates were then averaged to arrive at the final value of Ψ_c . The values of Ψ_c as a function of c at 150°C and 7 RPM are presented in Table 4.

A plot of Ψ_c vs. c was then made. A second order polynomial was used to fit the points. The result is shown in Figure 4.13. The functionality of Ψ_c and Ψ_{cc} for this particular case was found to be

$$\Psi_c(c) = 0.18 c^2 - 0.095 c + 0.02 \quad (4.8)$$

and

$$\Psi_{cc}(c) = 0.36 c - 0.095 \quad (4.9)$$

where c is in cm^2 , Ψ_c is in sec^{-1} and Ψ_{cc} (the second derivative of the stream function with respect to c) is in $\text{sec}^{-1}/\text{cm}^2$. The value of the constant c is always positive and is continuous in nature. The continuous nature of c is clearly demonstrated by Figure 4.13, hence the data obtained is justifiable. Also

TABLE 4.2

VALUES OF Ψ_c AS A FUNCTION OF c FOR
LLDPE AT 150 °C AND 7 RPM

Ψ_c, sec^{-1}	c, cm^2
0.00415	0.320
0.00560	0.376
0.00673	0.412
0.00830	0.420
0.00953	0.452
0.00835	0.422

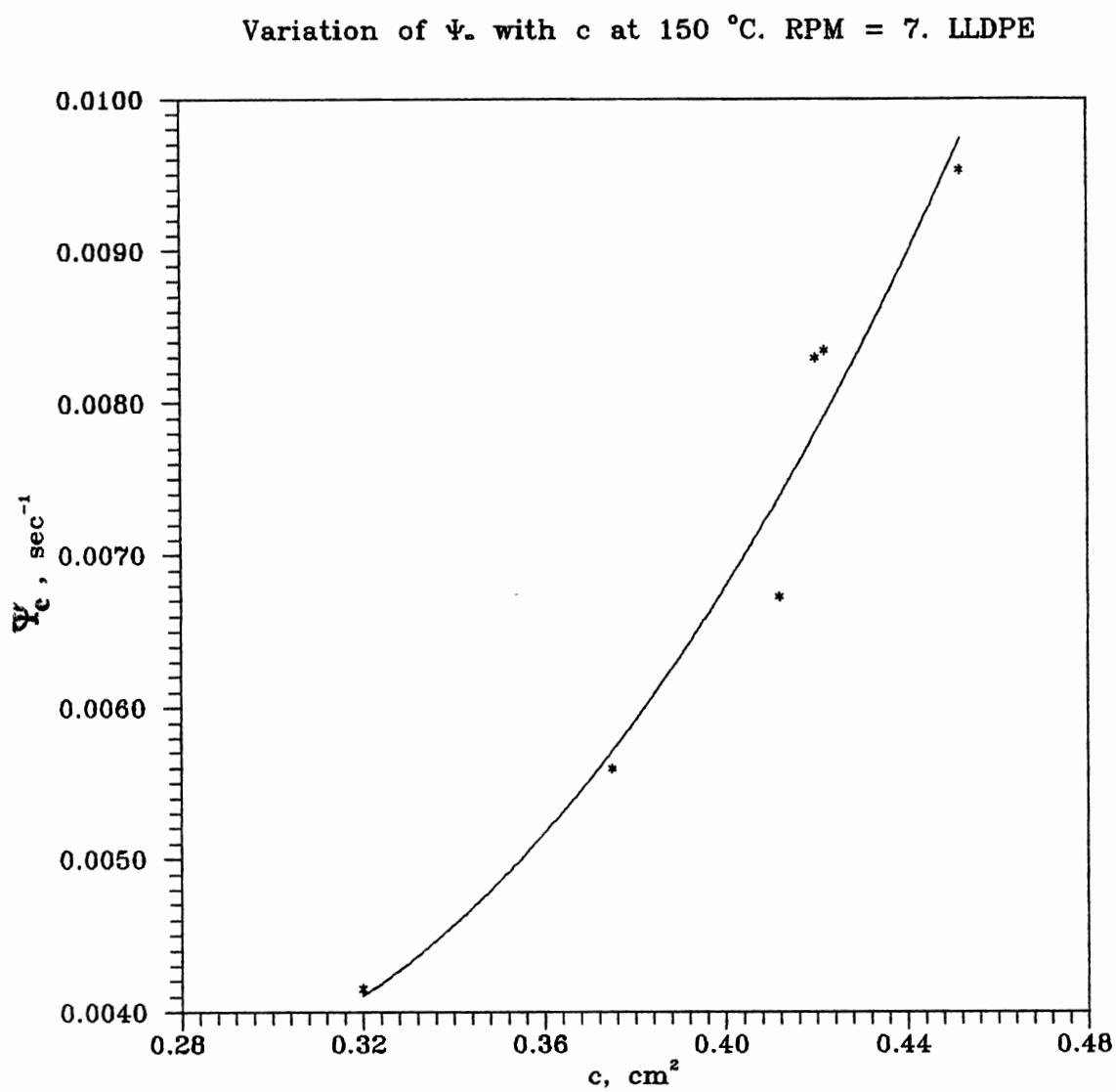


Figure 4.13: Ψ_c as a Function of c

the plot very closely follows all the data points further supporting the representation of the function. Thus an approach to characterization of the flow has been made. However, it should be mentioned that the fits applied are pertinent to this system only and further studies need to be conducted.

Using Equations 4.8 and 4.9, the velocities were calculated by substituting into Equations 2.14 and Equations 2.15 respectively for the individual components;

$$u_x = \frac{2y}{\sin^2\eta} [0.18c^2 - 0.095c + 0.02] \quad (4.10)$$

$$u_y = \frac{2x}{\cos^2\eta} [0.18c^2 - 0.095c + 0.02] \quad (4.11)$$

The x directed velocity component is found to increase while the y directed velocity decreases with distances away from the slit die entrance. The results obtained above are reasonable because at points near the center of flow, where η approaches 90° , η becomes the controlling factor, hence the y directed velocity increases. Conversely, near the walls with decreasing η , the distance from the center becomes the controlling factor. Also as it would have been expected the velocity increases as the particle approaches the slit die entrance. The behavior seen above is very much expected in order to satisfy the equations of motion.

The elongation rates were then calculated by substituting Equation 4.9 into Equation 2.22 to get the x-x and the y-y components respectively for the individual components as:

$$\dot{\gamma}_{xx} = -\dot{\gamma}_{yy} = \frac{8xy}{\sin^2\eta \cos^2\eta} [0.36c - 0.095] \quad (4.12)$$

Along each streamline the strain rates increased with distance from the slit entrance and as the center was approached from the top edge indicating that the diagonal components of the rate of strain tensors were more predominant than the non-diagonal components. The above statement can be explained on similar grounds as explained for the velocity components, that near the center the cosine term is the controlling factor while at points away from the center the sine term is the controlling factor. The result obtained is as expected and can be directly explained from the velocity behavior of the melt as: as the center of the flow is approached the x component decreases and approaches zero (as described earlier), thereby all the velocity contribution is primarily due to the y component, thus the flow is stretching or elongational in nature. Thus it could be inferred that as the center of the flow was approached or at a point sufficiently away from the entrance elongational flow behavior is attained.

All the above results go on to show that the function used to characterize the streamline is in good agreement with the actual behavior of the melt, and qualitatively accurate in describing the kinematics of flow of polymer melts in converging channels.

CHAPTER V

SUMMARY, CONCLUSIONS, AND RECOMMENDATIONS

Summary and Conclusions

This work was successful in exploring the possibilities of application of elliptical-cylindrical coordinates in heterogenous, mixed flow behavior of polymer melts in converging channel. The application of stress-optic relationship to their studies has been further confirmed. The results of this thesis can be summarized as:

1. Mixed, heterogenous flow of polymer melts was generated by appropriate design of the slit flow die, which is critical to the aim of this whole thesis.
2. The Method of Isoclinics was successfully used to measure the stress optic coefficients of LLDPE for the temperature range of 140 °C to 185 °C. The behavior of the SOC as a function of temperature was found to compare favorably with that available in the literature.
3. The Method of Isoclinics was successfully used in developing the shear stress and First Normal Stress Difference in the converging section of the die.
4. The ability of elliptical cylindrical coordinates to represent the streamfunction in the converging section of the die has been demonstrated.
5. From the stream function the non-zero components of the rate of strain

tensor have been derived.

6. The x and the y components of the velocity vector could be adequately described by the streamfunction, thereby leading to the conclusion that the function used is a good representation to describe the streamlines.

Recommendations

It is recommended that the heterogenous, mixed flow behavior of polymer melts in converging channels be further studied, specifically :

1. The leakage in the die can be eliminated to a large extent by usage of high temperature sealants or by using some gaskets.
2. Use of a retarder plate is recommended to clearly distinguish the isochromatic and the isoclinic bands in the slit and the converging section.
3. Calculations to relate the shear rate and their variation with the elongation rates.
4. Correlate the data obtained for shear stress and elongational stress from the birefringence technique with the shear and elongation rates obtained from using the stream function technique.
5. Further study on the mixed, heterogenous flow of polymer melts is recommended to arrive at an equation of state, which would adequately define this regime.

REFERENCES

1. I. M. Ward, "Structure and Properties of Oriented Polymers", John Wiley & Sons, NY (1975).
2. D. V. Boger and H. Nguyen, "A Model Viscoelastic Fluid," Polym. Eng. and Sci., 18, 1037 (1978).
3. C. D. Han and K. U. Kim, "A Comparison of Measurements of the Viscoelastic Properties of Polymer Melts by Means of the Han Slit/Capillary Rheometer and the Weissenberg Rheogoniometer," J. Appl. Polym. Sci., 17, 95 (1973).
4. F. N. Cogswell, "Converging Flow of Polymer Melts in Extrusion Dies," Polym. Eng. Sci., 12 (1), 64 (1972).
5. T. R. Fields, Jr. and D. C. Bogue, "Stress-Birefringent Patterns of a Sharp-Edged Entrance," Trans. of Society of Rheol., 12, 35 (68).
6. R. L. Boles, H. L. Davis, and D. C. Bogue, "Entrance Flow of Polymeric Materials: Pressure Drop and Flow Pattern," Polym. Eng. Sci., 10 (1), 24 (1970).
7. J. L. Duda, J. S. Vrentas, "Entrance Flows of Non-Newtonian Fluids," Trans. Soc. of Rheology, 17, 89 (1973).
8. L. H. Drexler and C. D. Han, "Studies of Converging Flows of Viscoelastic Polymeric Melts," J. Appld. Polym. Sci., 17, 2255 (1973).
9. T. H. Forsyth, "Converging Flow of Polymers," Polym. Plast. Technol. Eng., Converging Flow of Polymers, 6(1), 101 (1976).
10. F. N. Cogswell, "Converging Flow and Stretching Flow: A Compilation," J. Non-Newtonian Fluid Mech., 4, 23 (1978).
11. H. J. Yoo and C. D. Han, "Stress Distribution of Polymers in Extrusion through a Converging Die," J. Rheo., 25, 115 (1981).
12. M. M. Denn, in R.S. Rivlin(ed.), "The Mechanics of Viscoelastic Fluid," AMD-Vol 22, ASME, NY, 1977, 101.

13. C. D. Han, "Influence of Die Entry Angle on the Entrance Pressure Drop, Recoverable Elastic Energy, and Onset of Flow Instability in Polymer Melt Flow," J. Appl. Polym. Sci., 17, 1403 (1973).
14. D. G. Baird, M. D. Read, and R. D. Pike, "Comparison of Hole Pressure and Exit Pressure Methods for Measuring Polymer Melt Normal Stresses," Polym. Engr. and Sci., 26, 225 (1986).
15. T. Samurkas, R. G. Larson, and J. M. Dealy, "Strong Extensional and Shearing Flows of a Branched Polyethylene," J. Rheol., 33, 559 (1989)
16. A. G. Gibson and G. A. Williamson, "Shear and Extensional Flow of Reinforced Plastics in Injection Moulding," Polym. Engr. and Sci., 25, 980 (1985).
17. S. A. White and D. G. Baird, "Flow Visualization and Birefringence Studies on Planar Entry Flow of Polymer Melts," J. Non-Newt. Fluid Mech., 29, 245 (1988).
18. H. F. Mark et al., "Encyclopedia of Polymer Science and Engineering", Vol. 14, John Wiley and Sons, New York, 1988.
19. Timothy F. Ballenger and James L. White, "The Development of the Velocity Field in Polymer Melts in a Reservoir Approaching a Capillary Die," J. Appl. Polym. Sci., 15, 1949 (1971).
20. S. A. Khan and R. G. Larson, "Comparison of Simple Constitutive Equations for Polymer Melts in Shear and Biaxial and Uniaxial Extensions," J. Rheol., 31, 207 (1987).
21. Okubo and Hori, "Shear Stress at Wall and Mean Normal Stress Difference in Capillary Flow of Polymer Melts," J. Rheol., 25, 139 (1981).
22. C. D. Han, "Measurement of the Rheological Properties of Polymer Melts with Annular Rheometer," J. Appl. Polym. Sci., 18, 481 (1974).
23. J. J. C. Picot, D. R. Wilson, and R. Subramanian, Polymer Processing Society, 7th Annual meeting, Hamilton, Ontario, 1991.
24. E. B. Adams, J. C. Whitehead, and D. C. Bogue, "Stresses in a Viscoelastic Fluid in Converging and Diverging Flow," AIChE J., 11, 1026 (1965).
25. E. B. Bagley, "End Corrections in the Capillary Flow of Polyethylene," J. Appl. Phys., 28, 624 (1957).

26. J. W. Prados and F. N. Peebles, "Two-Dimensional Laminar-Flow Analysis, Utilizing a Doubly Refracting Liquid," *AIChE J.*, 5, 225 (1959).
27. C. D. Han and L. H. Drexler, "Studies of Converging Flow of Viscoelastic Polymer Melts," *J. Appl. Polym. Sci.*, 17, 2329 (1973).
28. C. D. Han, "Measurement of Stress Birefringence Patterns in Molten Polymers Flowing through Geometrically Complex Channels," *J. Appl. Polym. Sci.*, 19, 2403 (1975).
29. H. J. Yoo and C. D. Han, "Stress Distribution of Polymer Melts through a Converging Die," *J. Rheol.*, 25, 115 (1981).
30. A. J. McHugh, M. E. Mackay, and B. Khomami, "Measurement of Birefringence by the Method of Isoclinics," *J. Rheol.*, 31, 619 (1987).
31. Max Mark Frocht, "Photoelasticity", Vol. 1, John Wiley and Sons, inc., NY (1941).
32. A. J. Durelli and W. F. Riley, "Introduction to Photomechanics", Prentice Hall, Inc., (1965).
33. A. W. Hendry, "Photo-elastic Analysis", Permagon Press Ltd., First edition., (1966).
34. D. A. Tree, PhD Thesis, Uni. of Illinois at Urbana Champagne, 1990.
35. H. Janeschitz-Kriegl, "Polymer Melt Rheology and Flow Birefringence", Springer-Verlag, NY (1983).
36. J. L. Wales, "The application of Flow Birefringence to Rheological Studies of Polymer Melts", Delft University Press, The Netherlands (1976).
37. J. L. White, "Behavior of Concentrated Suspensions of Small Particles in Polymer Melts," *J. Non-Newt. Fluid Mech.*, 5, 177 (1979).
38. C. J. S. Petrie, "Extensional Flows of Oldroyd Fluids," *J. Non-Newt. Fluid Mech.*, 14, 189 (1984).
39. A. M. Hull and J. R. A. Pearson, "On the Converging Flows of Viscoelastic Fluids through Converging Channels," *J. Non-Newt. Fluid Mech.*, 14, 219 (1984).
41. M. Rallison and E. J. Hinch, "Do We Understand the Physics in the Constitutive Equations," *J Non-Newt. Fluid Mech.*, 29, 37 (1988).

42. C. D. Han, "Rheology in Polymer Processing", Academic Press, Inc., New York, 1976.
43. Humphry, R. H., Proc. Phys. Soc. (London), 35, 217 (1923); as cited in Prados and Peebles (26).
44. Alcock, E. D. and C. C. Sadron, Physics, 6, 92 (1935); as cited in Prados and Peebles (26).
45. Maxwell, J. C., Roy. Soc. (London), 22, 46 (1873); as cited in Prados and Peebles (26).
46. Rosenberg, Benjamin, Rept. (61), Navy Dept., David W. Taylor Model Basin, Washington 7, D. C., (1952).
47. Treloar, L. R. G, "The Physics of Rubber Elasticity", Third Edition, Clarendon Press, Oxford (1975).
48. Kuhn, W. and F. Grun, "Beziehungen zwischen elastischen konstanten und Dehnungsdoppelbrechung hochelastischer Stoffe," Kolloid Z., 101, 248 (1942); as cited in D. A. Tree (34).
49. Lodge, "The Isotropy of Gaussian Molecular Networks and the Stress Birefringence Relations for Rubber Materials Cross-Linked in Stressed States," Kolloid. Z., 171, 46 (1960); as cited in D. A. Tree (34).
50. Material Safety Data Sheet provided by the manufacturer, Quantum Chemicals, TX 77641.
51. Parry Moon and D. E. Spencer, "Field Theory for Engineers", D. Van Nostrand Company Inc., Princeton, N.J. (1961).
52. J. M. Dealy, "Extensional Flow of Non-Newtonian Fluids - A Review," Polym. Engr. Sci., 11, 433 (1971).
53. Hurlimann, H. P. and W. Khappe, "Der Zusammenhang zwischen der Dehnspannung von kunststoffschmelzen im Düsenlauf und im Schmelzbruch," Rheol. Acta, 11, 292 (1972) as cited in D. A. Tree (34).
54. C. Balakrishnan, Proc. VII Int. Congr. Rheology, Gothenburg, 1976, as cited in Cogswell (10).
55. D. R. Oliver, "The Prediction of Angle of Convergence for the Flow of Viscoelastic Liquids into Orifices," Chem. Eng. J., 6, 265 (1973).

56. Phillipoff, W and J. L. S. Waales, "The Anisotropy of Simple Shearing Flow," *Rheol. Acta*, 12, 25 (1973).
57. S. R. Galante and P. L. Frattini, "The influence of End Effects on Birefringence Measurements in nominally two-Dimensional Channel Flows," *J. Rheol.*, 35, 1551 (1990).
58. P. R. Schunk and L. E. Scriven, "Constitutive Equation for Modelling Mixed Extension and Shear in Polymer Solution Processing," *J. Rheol.*, 34, 1085 (1990)
59. P. D. Frayer and P. J. Huspeni, "Processing Preshear and Orientation Effects on the Rheology of an LCP Melt," *J. Rheol.*, 34, 1199 (1990).
60. S. Pilitsis, A. Souvaliotis, and A. N. Beris, "Viscoelastic Flow in a Periodically Constricted Tube: The combined effect of Inertia, Shear Thinning, and Elasticity," *J. Rheol.*, 35, 605 (1991).

APPENDIX A

NOMENCLATURE

NOMENCLATURE

b	channel half height
C	stress optic coefficient
c	a constant associated with the streamine
$N1$	First Normal Stress Difference
n_{p1}	first principle refractive index
n_{p2}	second principle refractive index
P	pressure
T	fraction of light transmitted
T	Temperature
t	present time
t'	past time
α	polarizer orientation angle
$\alpha_1 - \alpha_2$	polarizability difference along and at 90° to a link
η	Constant Coordinate value in Elliptical-Cylindrical Coordinates
γ	the rate of strain tensor
γ	major phase shear rate or extension rate
γ_{ij}	elements of rate of strain tensor
Δn	the birefringence
τ	the stress tensor
τ	shear stress

τ_{ij}	elements of the stress tensor
τ_{p1}	first principle stress
τ_{p2}	second principle stress
τ_{11}	first normal stress
τ_{12}, τ_{21}	shear stress
τ_{22}	second normal stress
τ_w	shear stress at the wall
τ_{xy}, τ_{yx}	shear stress
χ	isoclinic angle or a rotation angle
χ_M	the orientation angle of the stress tensor
χ_o	the orientation angle of the refractive index tensor
Ψ	the stream function
Ψ_c	the partial derivative of Ψ with respect to c
Ψ_{cc}	second partial derivative of Ψ with respect to c

APPENDIX B

STRESS OPTIC COEFFICIENT

TABLE B.1

STRESS OPTIC COEFFICIENT AT 140 °C

$\Delta n \cdot 10^5$	τ_{12} (psi)	$\tau_{11} - \tau_{22}$ (psi)
5.763	1.651	2.000
3.458	1.032	0.821
1.921	0.413	0.232
1.921	0.310	0.232
3.266	0.929	0.776
5.283	1.548	1.834
10.57	3.300	4.716
9.605	3.260	4.289
6.724	2.173	2.335
3.458	1.287	0.821
4.803	1.358	1.668
8.645	2.580	3.859
9.605	2.925	4.288
6.724	2.438	2.335
4.803	1.950	1.141
5.763	2.113	2.000
9.605	2.925	4.297
8.645	2.900	3.859
6.724	2.354	2.335
7.684	2.173	2.668

Material = Linear Low Density Polyethylene

TABLE B.2

STRESS OPTIC COEFFICIENT AT 150 °C

$\Delta n \cdot 10^5$	τ_{12} (psi)	$\tau_{11} - \tau_{22}$ (psi)
3.842	1.309	1.331
0.961	0.594	0.169
1.921	0.712	0.667
3.842	1.662	1.946
5.764	2.469	2.919
2.882	1.235	1.000
0.961	0.617	0.169
5.763	2.112	2.919
1.921	0.811	0.606
0.961	0.486	0.169
1.921	1.135	0.313
5.763	2.595	2.919
2.882	0.889	1.000
1.922	0.533	0.338
4.803	2.133	1.664
6.724	2.844	3.406
10.56	4.267	6.881

Material = Linear Low Density Polyethylene

TABLE B.3

STRESS OPTIC COEFFICIENT AT 170 °C

$\Delta n \sin(2\chi)/2 \cdot 10^5$	τ_{12} (psi)	$\tau_{11} - \tau_{22}$ (psi)
2.080	1.455	2.086
1.715	1.008	1.084
0.946	0.448	0.290
0.757	0.560	0.232
0.903	0.672	0.571
1.248	1.120	1.251
1.839	1.623	2.681
3.087	2.749	6.391
2.080	1.414	2.086
1.715	1.021	1.084
0.946	0.471	0.290
0.946	0.550	0.290
0.903	0.628	0.571
1.497	1.178	1.502
2.575	2.356	3.574
3.704	2.952	7.669
2.080	1.350	2.086
1.354	0.844	0.856
1.664	1.012	1.669
2.943	1.940	7.670

Material = Linear Low Density Polyethylene

APPENDIX C

MIXED FLOW KINEMATICS

TABLE C.1

DATA ALONG A PARTICULAR STREAMLINE AT $\eta = 78.1$

x(cm)	y(cm)	u_x (cm/sec)	u_y (cm/sec)	$\gamma_{xx} = -\gamma_{yy}$
0.101	0.000	0.0047	0.054	0.003
0.105	0.055	0.005	0.051	0.014
0.113	0.106	0.0055	0.048	0.028
0.121	0.143	0.0061	0.044	0.041
0.130	0.187	0.0066	0.040	0.057
0.137	0.227	0.0070	0.037	0.073
0.144	0.264	0.0074	0.037	0.090
0.152	0.301	0.0076	0.036	0.110
0.160	0.334	0.0077	0.035	0.126
0.165	0.367	0.0078	0.033	0.143
0.175	0.404	0.0078	0.032	0.160

Material = Linear Low Density Polyethylene

Temperature = 150 °C

RPM = 7

TABLE C.2

DATA ALONG A PARTICULAR STREAMLINE AT $\eta = 76.2$

x(cm)	y(cm)	u_x (cm/sec)	u_y (cm/sec)	$\gamma_{xx} = -\gamma_{yy}$
0.12	0.0332	0.005	0.048	0.007
0.125	0.066	0.006	0.045	0.015
0.133	0.106	0.007	0.042	0.025
0.143	0.147	0.0072	0.038	0.038
0.150	0.187	0.007	0.036	0.05
0.156	0.216	0.0074	0.034	0.06
0.163	0.246	0.0075	0.031	0.072
0.168	0.279	0.0075	0.030	0.084
0.173	0.308	0.0077	0.028	0.095
0.185	0.334	0.0077	0.028	0.111
0.189	0.363	0.0080	0.026	0.123

Material = Linear Low Density Polyethylene

Temperature = 150 °C

RPM = 7

TABLE C.3

DATA ALONG A PARTICULAR STREAMLINE AT $\eta = 85.4$

x(cm)	y(cm)	u_x (cm/sec)	u_y (cm/sec)	$\gamma_{xx} = -\gamma_{yy}$
0.039	0.029	0.0030	0.078	0.017
0.042	0.100	0.0035	0.072	0.063
0.048	0.172	0.0037	0.066	0.124
0.052	0.238	0.0038	0.059	0.186
0.055	0.297	0.0039	0.055	0.245
0.058	0.352	0.0040	0.052	0.307
0.062	0.404	0.0042	0.048	0.376
0.065	0.448	0.0043	0.045	0.437
0.07	0.495	0.0043	0.043	0.521

Material = Linear Low Density Polyethylene

Temperature = 150 °C

RPM = 7

TABLE C.4

DATA ALONG A PARTICULAR STREAMLINE AT $\eta = 78.5$

x (cm)	y (cm)	u_x (cm/sec)	u_y (cm/sec)	$\gamma_{xx} = -\gamma_{yy}$
0.097	0.092	0.0065	0.051	0.022
0.104	0.143	0.0067	0.05	0.037
0.113	0.191	0.0069	0.047	0.054
0.120	0.238	0.0070	0.041	0.072
0.126	0.279	0.0071	0.040	0.088
0.133	0.319	0.0072	0.037	0.110
0.139	0.345	0.0074	0.036	0.124
0.144	0.389	0.0074	0.034	0.142
0.152	0.426	0.0074	0.033	0.163

Material = Linear Low Density Polyethylene

Temperature = 150 °C

RPM = 7

TABLE C.5

DATA ALONG A PARTICULAR STREAMLINE AT $\eta = 81.1$

x (cm)	y (cm)	u_x (cm/sec)	u_y (cm/sec)	$\gamma_{xx} = -\gamma_{yy}$
0.073	-0.070	0.000	0.075	0.00
0.074	0.003	0.0055	0.073	0.009
0.082	0.081	0.0058	0.062	0.027
0.092	0.143	0.0060	0.057	0.054
0.099	0.202	0.0065	0.053	0.082
0.104	0.246	0.0068	0.048	0.105
0.110	0.301	0.0071	0.044	0.136
0.116	0.345	0.0073	0.041	0.164
0.124	0.389	0.0075	0.038	0.198
0.132	0.426	0.0076	0.036	0.231
0.137	0.462	0.0076	0.035	0.260

Material = Linear Low Density Polyethylene

Temperature = 150 °C

RPM = 7

TABLE C.6

DATA ALONG A PARTICULAR STREAMLINE AT $\eta = 82.6$

x (cm)	y (cm)	u_x (cm/sec)	u_y (cm/sec)	$\gamma_{xx} = -\gamma_{yy}$
0.063	- 0.018	0.000	0.076	0.000
0.066	0.055	0.005	0.073	0.0214
0.072	0.117	0.0055	0.066	0.050
0.079	0.183	0.0059	0.052	0.085
0.087	0.235	0.0064	0.051	0.120
0.092	0.286	0.0068	0.048	0.155
0.095	0.334	0.0071	0.044	0.187
0.103	0.378	0.0073	0.042	0.229
0.107	0.422	0.0074	0.040	0.266
0.113	0.470	0.0074	0.037	0.313

Material = Linear Low Density Polyethylene

Temperature = 150 °C

RPM = 7

APPENDIX D

DESIGN CONSIDERATIONS OF THE DIE

DESIGN CONSIDERATIONS OF THE SLIT FLOW DIE

The design of the die was crucial to the aim of the thesis, hence it was essential that certain considerations were made during the design of the die:

1. The die had to be designed, keeping in mind that the data for stress optic coefficients were to be generated before the stress field in the converging section could be examined.

The stress optic coefficient of a polymer melt at a specific temperature can be obtained provided we have a knowledge of the shear stress, the birefringence, and the isoclinic angle. Since the birefringence and the isoclinic angles are obtained from birefringence techniques the shear stress in this section need to be quantified. However, in a fully developed flow the shear stress acting at any point in the flow field could be computed from the equations of motion. A fully developed flow is thus essential and could be obtained in the slit flow section. Thus pressure transducers were mounted flush in the slit flow section equidistant to each other. The linearity of the pressure gradient could thus be used as a check to see if the flow was fully developed. To meet the same criteria a point sufficiently away from the slit die entrance was chosen.

In order to check if the pressure transducers were mounted flush in the slit, one of the transducers was mounted such that it could be seen through the window. The middle transducer could also used to measure the melt

temperature in the slit section.

2. In the converging section, a mixed, heterogenous flow was obtained by constraining the melt to flow through a converging channel such that near pure shear forces were present near the walls while elongational forces dominated near the center. In between is a region of both shear and extension forces acting simultaneously, the rate of deformation in each case being different at different positions in the die. Thus a mixed, heterogenous flow could be obtained in the converging section.

The angle of the converging section could be varied by removing the brass notch and replacing it by another similar one of the desired angle. The convergence angle should be kept lesser than the natural flow convergence angle of the polymer melt so as to avoid vortex formation.

3. The stresses in the converging section were to be obtained by using the birefringence technique, for which the position of the isoclinic bands is essential. Due to the larger area of the converging section and for larger viewing section, windows of 2 in. diameter were employed. While positioning the window in the converging section care was also taken to see that a part of the slit section was seen to get a feel for the rapidity with which the flow would attain a steady profile after entering the slit section.

4. The kinematics in the mixed flow regime were to be obtained by using the tracer particle technique. For this procedure a larger viewing area was required to trace the path of the particles in the converging section. Also the path traced by the particles once they entered the slit section would be of some

interest. Hence a window with a larger viewing area was employed.

5. The temperature of the die was to be maintained constant during the course of the experiment, hence the die was to be wound and heated by insulated fiberglass tapes. The temperature of the die was to be maintained constant by a feed back control from the die hence a thermocouple well was provided. To prevent loss of heat, the die was made up of stainless steel because steel has very low thermal conductivity. However, to prevent further loss of heat the die was to be covered by ceramic wool insulators. The insulators also prevented any harm due to accidental human contact with the surface of the die.

6. The aspect ratio, ratio of width to the height of the channel, should be kept sufficiently high so that the two dimensionality condition is approximately satisfied.

7. The reservoir section of the die, just prior to the converging notch is kept sufficiently large so that a uniform flow could be obtained. A larger reservoir section is also essential to dampen the spiralling flow induced by the screw.

8. Teflon gaskets were employed to prevent any leakage between the windows and the die. The gaskets helped in cushioning the windows against the walls and also prevented any scratches on the window.

APPENDIX E

APPARATUS DESCRIPTION

APPARATUS DESCRIPTION

The apparatus used in the study of mixed, heterogenous flow is shown in Figure E.1. The apparatus comprises primarily of an extruder, a die, an optical set up, and a fume hood.

The blue panel seen in the right side of the picture is the control panel of the extruder. The extruder was a Killion extruder with a 1 in. screw (model number KLB-100). The temperatures in the die, adapter, and the different zones of the extruder were controlled by five switches located on the panel, as seen in the picture. The screw was run with the help of reduction gears and the speed controlled with the help of a potentiometer. The speed of the motor could be directly read out from the tachometer on the panel.

The hopper through which the polymer is fed is seen in the front portion of the picture. The polymer pellets or powder was fed through the hopper and heated as they passed through the barrel of the extruder. The extruder barrel was inside the silver rectangular housing adjacent to the hopper. The temperature in different zones of the die were controlled with the help of a feed back control. The pressure in the extruder barrel could be measured from the pressure indicator and the melt temperature measured using a thermocouple at the end of the barrel. The different zones of the extruder could be cooled with three fans.

The extruder was connected to the die. The free end of the die was

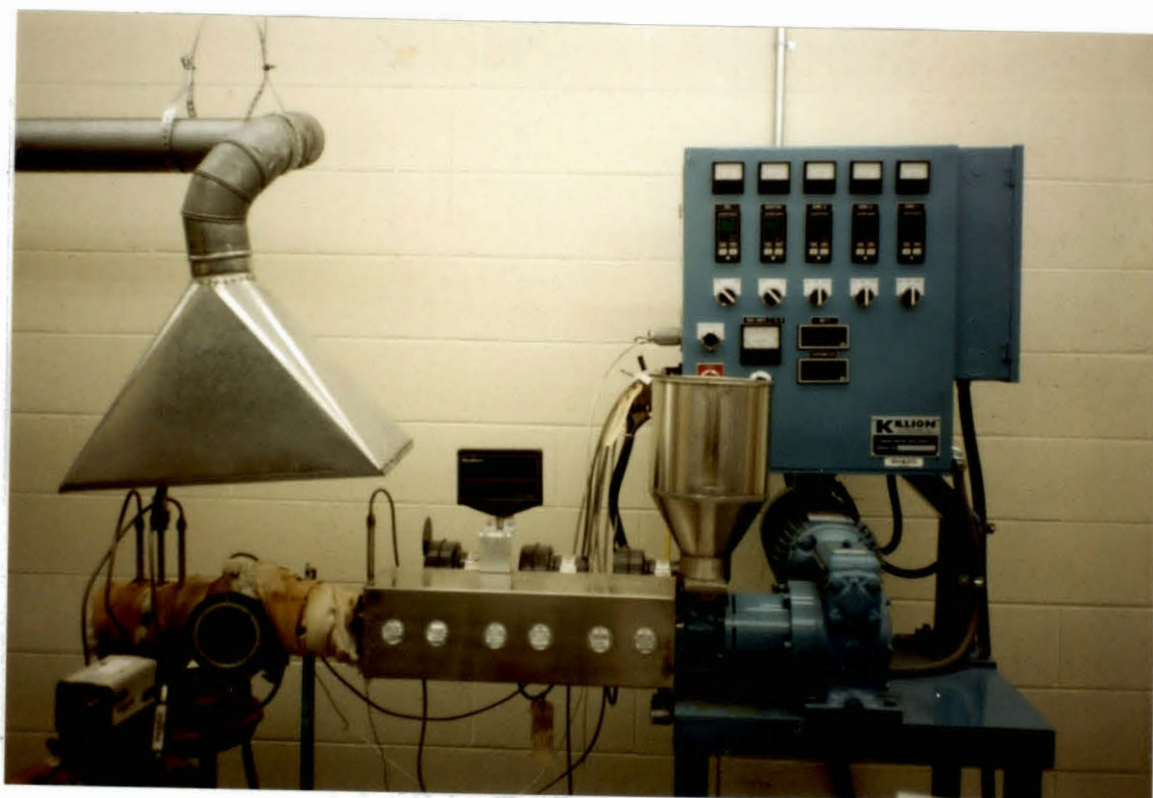


Figure E.1: Apparatus Setup

supported by a suitable support. The die was wrapped with heating coils, and the heating controlled by feed back mechanism from the extruder. To prevent loss of heat, the die was insulated with ceramic wool insulations. The insulators also prevented any harm due to accidental human contact with the surface of the die. Three pressure transducers were installed in the die and connected to a pressure transducer, to measure the pressures. The region between the extruder and the die were heated with the help of an adapter to prevent any freezing of the polymer while it moved from the extruder to the die.

The light traversing through the front windows passes through the analyzer, seen as a black circular frame in front of the die, which was recorded by the video camera. The camera is connected to a monitor and a VCR for recording the flow of the melt in the different sections of the die.

A fume hood was installed to remove the fumes emanating from the die, when it was heated, which could cause irritation.

VITA²

SUNIL SINGH AJAI

Candidate for the Degree of

Master of Science

Thesis: STUDY OF MIXED, HETEROGENOUS FLOW KINEMATICS OF
POLYMER MELTS IN CONVERGING CHANNELS

Major Field: Chemical Engineering

Bibliographical:

Personal Data: Born in Jodhpur, India, November 5, 1968, son of
Ajai Shanker Singh and Damayanti Devi.

Education: Received Bachelor of Science Degree in Chemical Engineering
from Bharatiar University at Coimbatore in June, 1990; completed
requirements for the Master of Science degree at Oklahoma State
University in December, 1992.

Personal Experience: Junior Engineer, East India Distilleries, April, 1990, to
August, 1990. Teaching Assistant, Department of Chemical Engineering,
August, 1990, to May, 1991. Research Assistant, Department of
Chemical Engineering, Oklahoma State University, June, 1991, and July,
1991. Teaching Assistant, Department of Chemical Engineering,
Oklahoma State University, August, 1991, to December, 1991.
Technical Assistant, Department of Biochemistry, January 1992, to July,
1992.